CHAPTER 9: ANALYSIS AND DISCUSSION

9.1 INTRODUCTION

It has been shown in the previous Chapters that the numerical modelling has been unable to adequately simulate the behaviour of the externally loaded buried pipes with the assumption of a laterally restrained sidewall. The step from two- to three-dimensional modelling made significant improvements to the simulations. However the most significant improvements arose after the sidewall boundary condition was investigated, and subsequently, boundary conditions were relaxed and the wall was provided with a realistic and finite stiffness (series 5 and subsequent analyses).

This Chapter makes a general review of the test data with particular attention given to the related literature as discussed in Chapter 2. A review of the finite element modelling is then made and recommendations for future laboratory testing and finite element modelling of buried pipes of similar pipe stiffness are given. Simple design guidelines follow for buried flexible pipes.

9.2 REVIEW OF BURIED PIPE TEST DATA

Data from the pressure cells provided an insight into the accuracy and reliability of the various non-numerical models for evaluating pipe deflections. Most of these models for pipe deformations allow estimation of vertical pipe deflection for plane strain conditions, based on the assumed pressure above the pipe crown (e.g. Watkins, 1988 and Molin, 1981). The geotechnical problem remains as to what pressure exists above the crown due to either dead (weight of backfill) or live load (trafficking of backfill surface). Section 9.2.1 examines the load spreading achieved in the non-paved, buried pipe tests.

The non-numerical methods require an evaluation of the sidefill (or surround) stiffness. The Spangler modulus or modulus of soil reaction, E′, has been adopted by many authors (refer equations 2-10 to 2-12). However it is not a simple soil material

property, as it is linked to pipe diameter and stress state. Section 9.2.2 reviews the experimental data in terms of this modulus. In the following section, the pressure cell data are interpreted to evaluate E′ and its variation throughout the test installations.

In the tests reported in this thesis, backfill weight was relatively insignificant and so in the ensuing discussion, all pressure cell data were relative to the start of testing and do not include stresses developed during installation. Likewise, diametric pipe strains measured during installation were ignored.

9.2.1 Load Spreading

In Chapter 2, it was revealed that AS/NZS 1988 advocated a simple geometric load spreading device for estimation of vertical soil pressures; the average vertical pressure at any depth below a loaded area could be evaluated on the basis of the hypothetical (effective) load area at depth. Elastic stress distribution analysis could have been applied (e.g. Holl, 1940). A comparison between the two approaches is provided in Figure 9-1. In the Figure, relative depth is given as the depth, z, below the loaded area, divided by the breadth of the loaded area, B. The stress reduction factor is the vertical stress at depth z, divided by the applied surface pressure, p. It is clearly evident that the AS/NZS 1988 recommendation is non-conservative with respect to Holl's solution, which is based on the theory of elasticity, over the depth of covers employed in this test series. The ratio of height of cover to the breadth of the loading plate, H/B, ranged between 1.5 and 4 for the non-paved tests, conducted with the 200 mm wide and 500 mm long, rigid plate.

In the tests, load spreading was seen to be a function of the height of soil cover, H, the level of applied pressure and the soil density. The reduction in vertical stress between the applied surface pressure and the earth pressure, $\sigma_{v@150}$, at 150 mm above and central to the crown of the pipe, has been plotted against the applied average surface pressure, p, in Figure 9-2 for the five backfill cover heights. The theoretical stress reduction due to the elastic stress distribution (Holl, 1940) has been included on each plot. The parameter, z, in the Figure is the depth below the surface at which the pressure cell was located.

It is apparent that the elastic solution for a semi-infinite, homogeneous and isotropic soil, underestimates the actual stress developed near the pipe crown in either the simulated trench, or in trenches excavated in a clay soil profile (i.e. the field tests). During the early stages of loading, in all but one case (test 450/5), the stress measured above the pipe was greater than the stress estimated using the Holl solution. With further loading, the difference between the measured and estimated stresses increased at an almost linear rate (except in test 300/1, in which a decrease was observed).

One explanation for this increase is the reduction of the effective cover height to the pipe as a consequence of the large plate settlements observed during the test. Examples of the influence of the change in height of cover on the elastic analyses for each of the five different initial cover heights are provided in the plots in Figure 9-2 (refer curves named, "Holl with current H"). Although this correction improves the agreement between observed and estimated values, particularly for F450/3, it can be concluded that an elastic approach for the trench condition can still be expected to significantly underestimate the earth pressure developed above the pipe.

9.2.2 Modulus of Soil Reaction, E′

Adopting the original definition of E′ as the modulus of soil reaction of the sidefill, values of this modulus may be determined from the data in tests, where pressure cells were located with their active faces opposite the springline of the pipe. The modulus of soil reaction is then simply the horizontal earth pressure divided by the lateral diametric strain. As the earth pressure was recorded a maximum of one pipe radius away from the pipe, an adjustment needs to be made for the pressure expected adjacent to the pipe. The adjustment was based on the theoretical stress distribution below a point load and could be expressed by a multiplying correction factor, T, where T is defined by the equation:

$$T = \left(\frac{r}{r_o} \right)^2 \qquad 9\text{-}1$$

where r = the distance between the pressure cell and the centre of the pipe

and r_o = the radius of the pipe

The equation assumes that the lateral increase of the pipe radius is caused by an equivalent horizontal force, which acts through the centre of the pipe. In elastic cylindrical cavity problems it is found that the stresses vary with the inverse square of the distance from the centreline of the cavity. It should be unsurprising therefore to discover that the adopted correction term, which reflects the radial offset of the stress measurement point from the pipe centreline, varies with the square of the distance from the centreline of the pipe

The average estimate of Spangler's modulus was calculated for ten of the buried pipe tests, which included two field tests. One estimate of the modulus appeared to be particularly low, just 1.9 MPa for test 300/8. As this test was essentially a repeat of 300/7 with almost identical soil density indices and load-deflection behaviour during testing, the estimate could not be justified. The only plausible explanation seemed to be that the cell numbers buried in the surround had been wrongly assigned to the cells with a vertical or horizontal active face (as was suggested in Chapter 8). By switching the pressure cell data between the two cells in the surround soil, Spangler's modulus, E′, increased by 215%. The estimates of E′ corrected for radial distance of the cell from the pipe centre, changed from 4.5 MPa to 9.6 MPa. Notably, this decision brought the estimate of E′ just 0.2 MPa greater than that realized in test 300/7. Subsequently the correction to the pressure cell data has been adopted in all future discussion in this thesis.

The uncorrected moduli (i.e., no correction applied for the finite distance of the measuring cell to the pipe wall) for the ten tests have been plotted in Figure 9-3a, against the initial density index of the surround. In this plot, the design recommendations of AS/NZS2566.1-1998 for the modulus of soil reaction have been imposed. It is evident that the exponential trendline to the data mirrored the expected increase of E′ with soil density provided by the Standard. However, the back-calculated values were less than the design recommendations of the Australian/New Zealand Standard.

Applying the correction to the modulus of soil reaction data, as expressed by equation 9-1, resulted in the revised plot in Figure 9-3b. Generally the new data

points fell either, on or above the line, which expressed the recommendations of AS/NZS2566.1-1998. The major divergences from this line were the two highest corrected values, which were related to the two field tests. For the field tests, the stiff to very stiff clay forming the trench walls would have increased the effective modulus when compared with E′ for a trench sufficiently wide that the influence of the side soil could be ignored.

As discussed in Chapter 4, the measured undrained soil Young's moduli of the natural clay soil varied between 30 and 95 MPa across the site. Generally, higher values of soil Young's modulus were recorded near the 450 mm diameter pipes. Leonhardt's correction factors were determined for the two pipe installations from the back-calculated moduli of soil reaction, assuming the Young's modulus of the natural soil, E_3, was 30 MPa for the 375 mm pipe test and 95 MPa for the 450 mm pipe test.

In order to get the data point in Figure 9-3b corresponding to test F450/3 close to the AS/NZS2566.1-1998 line, a Leonhardt correction factor of 2.58 is required, which corresponds to a value of 8.5 MPa for the sidefill modulus of soil reaction. For test F375/7 a Leonhardt correction factor of 3.64 is required to match a slightly extrapolated AS/NZS value of 17.5 MPa at a density index of 85%. This required value of the correction factor exceeds the maximum possible value of 2.3, suggesting either an error in the measurements or inadequacy of the Leonhardt factor. Problems were encountered in this test when taking measurements of the horizontal pipe movements, and so the back-calculated value of E′ should be adopted with considerable caution.

In summary, it would appear that the recommendations of AS/NZS2566.1-1998 regarding the variation of the modulus of soil reaction for a poorly graded sand and variation of the modulus with soil density index are reasonable for design purposes for shallow pipe burials.

9.2.3 Young's Modulus of the Soil, E

In order to assess the Young's modulus of the sand, the analyses of the two plate loading tests, as described in Chapter 6, were re-visited. FEA were conducted using

an elastic and isotropic soil mass to find the typical constant Young's modulus of the soil for the density at which it was prepared, namely a density index of 75%. A Poisson's ratio of 0.25 was adopted for the sand. The interface between the drum walls and the sand was modelled with an interface joint as previously. The results of these analyses are presented in Figure 9-4.

In the early stages of loading, the load deflection test data were well represented by a Young's modulus of 6 MPa (ELAS 6), but as the sand stiffened with loading, a modulus of 6.5 MPa was seen to be more appropriate. Adopting Watkins (1988) proposal that the modulus of soil reaction, E′, is equivalent to the constrained or bulk modulus, M, of a vertically loaded soil, then for a Poisson's ratio of 0.25, E′ = 1.2E (refer equation 2-38). Therefore the back-calculated values of E′ ranged between 7.2 and 7.8 MPa. This range has been plotted on Figure 9-3b ("plate loading test"). It is evident that the back-calculated values of E′ are somewhat lower than those promulgated by AS/NZS2566.1-1998 (interpolated value of 10.5 MPa at a density index of 75%).

9.2.4 Backcalculated Values of Young's Modulus of Sidefill using Hoeg's Theory

As discussed in Chapter 2, Hoeg (1968) proposed that the deflections of a pipe could be determined if the far field stresses were known. Although this theory is strictly only applicable to embankment loadings, it was applied to this particular loading condition, a patch load on the surface of the backfill from the wheels of a heavy vehicle. As in the FEA, the interface between the pipe and the soil was assumed to be perfectly rough.

The influence of the ratio of the horizontal to the vertical stresses in the soil, K, was investigated. Ratio K is assumed to be constant over the full range of loading. Values of Poisson's ratio for the soil were carefully chosen to be compatible with both the soil's Young's modulus and bulk modulus, and the soil pressure ratio, K.

The variation of the ratio, K, observed in the tests was examined by comparing the measured pressures horizontally in the surround and vertically at a height of 150 mm above the pipe crown over the full range of test loading. The results have been

presented in Figure 9-5. There did not appear to be any pattern to the values of K observed in each test, with respect to either the initial height of backfill cover, or the density index of the sand in the surround (values in % are given in the legend). For the laboratory tests, K ranged between 0.15 and 0.55 in the early stages of loading, i.e. below a vertical pressure of 250 kPa above the pipe crown.

Data from the two field tests bounded the laboratory test data. The field test on the 375 mm pipe produced the highest K ratios while the test on the 450 mm diameter pipe yielded the lowest values. Both the field tests displayed relative unloading of the surround soil as the loading on the surface of the backfill was increased, suggesting that arching was ineffective. Only tests 450/1 and 2 in the laboratory test series demonstrated similar behaviour. Of these four tests, three concerned 450 mm diameter pipes, the pipe in the series of tests with the least stiffness (S = 1 kPa).

In applying Hoeg's theory, the chosen values of K ranged between 0.2 and 0.5, which corresponded to a range of Poisson's ratio of the sand of 0.17 to 0.33. Young's moduli were selected to give vertical pipe deflections which best matched the experimental data. The matching of predicted and observed pipe deflection data is presented in Figures 9-6 to 9-10.

The combinations of Young's modulus and soil pressure ratio, which gave the best correspondence with the vertical deflection of the pipe and pressure cell data, are presented in Table 9-1. Although the combinations of E and K for any one test appeared to vary widely and could affect the predicted lateral response of the pipe to loading, when the elastic parameters were converted to a modulus of soil reaction, E′, by assuming that E′ is identical to the one-dimensional constrained modulus (equation 2-38), it was found E′ varied little for each test. For example, E′ varied between 28 and 30 MPa for the three combinations of E and K shown for test 300/5 in Figure 9-6b.

It should be noted that the lateral pipe deflections were often significantly underestimated by Hoeg's theory, although the two field tests and tests 450/1 and 2 were adequately simulated (Figures 9-9 and 9-10). Although the experimental lateral

pipe diametric strains were less than the vertical pipe deflections generally, they were not as low as those predicted by Hoeg's theory.

The data on modulus of soil reaction from Table 9-I were plotted against density index in Figure 9-11. The trend line for the data suggested an almost linear relationship between E′ and density index of the sand. However the predicted values of the modulus of soil reaction were generally significantly greater (up to two to three times) than the corrected values of E′ reported in Figure 9-3b, which were based directly on the experimental pressure and deflection data. For example, at a density index of 70%, the four back-calculated values ranged between 18 and 28 MPa, while the corresponding data from Figure 9-3b indicated a variation from just 6.7 to 10.9 MPa. The back-analysis of the plate loading test suggested E′ should be a maximum of 7.8 MPa at a density index of 75%, however the two values back-calculated on the basis of Hoeg's theory were much greater at 11 and 27 MPa.

In the lower diagram in Figure 9-11, the constrained modulus values derived from Moore (2001) of Table 2-III have been superimposed for vertical pressures ranging between 7 and 140 kPa. Although the maximum density index is only 70% in Table 2-III, good correspondence with the backcalculated values is evident. The difficulty remains for designers to correctly choose the design vertical pressure, which is relatively simple for embankment loading conditions, but is problematic for traffic loading. In these shallow buried pipe installations, the dead load vertical pressure after installation at the level of the springline was estimated to have varied between only 7 and 16.5 kPa.

It may be concluded that the estimates of the modulus of soil reaction based on application of Hoeg's theory and matching of the measured pressures at two points within the soil with pipe strain measurements, appeared to lead to overestimation of the modulus for the range of density indices considered. This outcome is perhaps not surprising, given that Hoeg's theory was developed for dead loading of buried pipes and the experimental data considered here were obtained from live load tests. It may also be concluded that the recommendations of AS/NZS2566.1-1998 underestimate

the modulus of soil reaction, when compared with the values from Moore (2001) for granular material at low levels of vertical stress.

9.2.5 Estimates of Pipe Deflections based on the Backcalculated Values of E′

The reliability of the estimates of the modulus of soil reaction, based on the soil pressure cell data and the lateral pipe deflection records, was checked by using the estimates of E′ from section 9.2.2 with the pipe deflection equations of Iowa (equation 2-12) and Watkins (equation 2-13). The vertical load on the pipe was taken to be the recorded soil pressure 150 mm above the crown and immediately below the centre of the loading plate. The estimated and observed vertical pipe deflections were compared and have subsequently been presented graphically in Figures 9-12 to 9-17. Both the Iowa and Watkins' equations predicted a linear increase of diametric strain with loading. The lateral diametric strains are assumed to be the same magnitude as the vertical strains by these two approaches.

Using the measured vertical soil pressures, together with the values of E′ from section 9.2.2, corrected for distance from the pipe, the Iowa equation successfully estimated the vertical pipe deflection for test 300/6, but overestimated deflections for tests 300/4, 5, 7 and 8 by as much as 70%. Test 300/6 afforded the greatest protection to the pipe, having 800 mm of cover above the pipe crown.

Predictions using the Iowa equation for the 375 mm diameter pipes were reasonable although the estimate for the field test, F375/7, was lower than the observed behaviour. As previously explained in section 9.2.2, this test was not completely successful and the effective modulus of soil reaction appeared to be too high.

The mixed success of the predictions of deflection using the Iowa equation continued with the 450 mm diameter pipes; the vertical pipe deflections in the field test, F450/3, were adequately predicted, but the laboratory tests, 450/1 and 2 were overestimated by approximately 100% in the early stages of the tests.

Watkins' empirical equation resulted in better predictions overall, but most notably for the 300 mm pipes (with 650 mm of cover) and the 450 mm diameter pipes. As

discussed in Chapter 2, Watkin's formula curtails high predictions of deflections when the ring stiffness ratio (E′/S) is high. The lowest value of ring stiffness was 4,660 for test 300/7, based on the corrected value of E′ of 9.4 MPa. Referring to Figure 2-7, Watkins' relationship indicates that above a ring stiffness ratio of 300, the vertical diametric pipe strain is more than 90% of the soil strain as expressed by (p_v/E′), which effectively means that the pipe stiffness contributes little to the control of deflections at high ring stiffness ratios. Above a value of 6000, the pipe strain is predicted to equal the soil strain.

For the ranges of pipe stiffness and modulus of soil reaction (E′) encountered in the tests in this thesis, Watkins hypothesized that "the vertical soil strain" should be equal to or greater than the vertical diametric strain of the pipe. To investigate this suggestion, the vertical soil strain was calculated as the soil pressure measured 150 mm above the pipe crown, divided by the back-calculated and corrected value of E′ for the installation (from Figure 9-3b). Then the soil strain estimates were compared with the measured vertical diametric pipe strains. The data have been plotted in Figure 9-18.

Reasonably linear responses are clearly evident between the pipe strain and the soil strain. The soil strain was greater than the vertical diametric pipe strain for most tests, except for the two laboratory tests on 450 mm diameter pipe with 450 mm of cover. On average the measured vertical pipe strain was 25% greater than the estimated vertical soil strain for these two tests.

The two field tests displayed the least vertical diametric pipe strain relative to the estimated soil strain.

9.3 REVIEW OF 3D FEA

In this section, the discussion is restricted to the analyses of the field tests, as in these tests the sidewall boundary conditions were comparatively obvious.

In Chapter 8, observations on the vertical soil pressure 150 mm above the pipe crown and at x = 0 were compared with finite element predictions and it was seen that the FEA yielded reasonable predictions of this pressure and consequently the vertical load-deflection behaviour of the pipe, despite being unable to model the plate settlement that occurred above a surface pressure of 300 kPa or so. However the pressure above the pipe crown was not uniform with distance, x, across the pipe. Most estimates of pipe deflections require the average pressure above the pipe over the pipe diameter and so the distribution of vertical pressure with distance was investigated. The distribution of the lateral pressure in the surround was also investigated. The results of these investigations are summarized in Figures 9-19 to 22. In these Figures, the soil pressure has been normalized, by dividing both the vertical and lateral pressure by the average applied surface pressure. As well, both the distance along the x-axis and the height above the base of the pipe have been normalized by dividing by the outer radius of the pipe.

The predicted patterns of development of soil pressure were similar between the four analyses. The vertical soil pressure 150 mm above the pipe crown tended to be concentrated in a distance from the centre of the pipe of less than one half radius, particularly as the applied surface pressure and the plate displacement increased. This distance was approximately 20% less for the FEA of the two 450 mm diameter pipe tests. However it should be noted that the concentration of pressure would also be related to the width of the surface loading, which was constant throughout these tests. The maximum extent of the vertical pressure reaching the soil above the pipe varied between tests from approximately 30 to 60% of the applied surface pressure. Of course these differences could be attributed largely to the differences in cover height adopted in the test; test F300/3 with only 450 mm of cover was predicted to experience the greatest transfer of stress from the surface of the backfill.

The lateral soil pressure distributions from the FEA of all four tests were also similar in shape to each other. Generally the peak lateral pressure in the centre of the surround occurred just above the springline in the early stages of loading, but thereafter was predicted to advance with loading past the top quarterpoint of the pipe (radial height of 1.5). Again the maximum extent of the lateral pressure for any one analysis varied with the installation geometry; the FEA of test F300/3 predicted the

greatest ratio of lateral pressure to applied surface pressure (approximately 0.3) of all the analyses.

A markedly different vertical pressure distribution was predicted closer to the pipe crown and for some methods of estimating pipe movement, this pressure distribution should be applied (e.g. Iowa equation, but not Hoeg's method). The soil pressure distribution was re-examined at the level of the first Gauss point above the pipe crown, and at the end of the finite element analysis, or at a surface displacement of 40 mm. The plots for the FEA of the field tests with the least and greatest cover, F300/3 and 375/7 respectively, are given in Figure 9-23. The full lines correspond to pressures 150 mm above the pipe crown, while the dashed line plots represent the predicted pressures nearer the crown.

It is evident from the plots that pressure has been re-distributed from the crown towards the outer area above, but inside, the springline. However the average vertical pressures between the two locations did not differ as much as might have been expected. The average vertical pressures at both levels above the pipe and over a distance equal to the pipe radius are provided in Table 9-II for all tests, at the end of each analysis. The average pressure 150 mm above the pipe varied between 100 and 137 % of the average pressure closer to the crown. The average variation was +14%.

The development with applied loading of the average vertical pressure 150 mm above the crown was found to be linear, after the surface pressure reached a certain value. The average pressure predicted in the soil above the pipe has been plotted against the applied surface pressure in Figure 9-24 for seven finite element analyses of field installations. The four simulated tests have been backed up with data from three fictitious field tests, extending the predictions for further combinations of installation geometry and pipe diameter. The extra analyses are referred to as F3700 (300 mm, 90VX pipe, with 700 mm of cover), F3745 (375 mm pipe with 450 mm of cover) and F4545 (450 mm pipe with 450 mm of cover). All extra analyses were performed with all the soil having an initial density index of 75%.

The value of pressure that was needed to reach linearity was expected to depend mainly on installation geometry as it would be a function of the maximum shear force able to be mobilized between the sand backfill and the natural clay walls of the trench. For example, the value of this pressure was approximately 150 kPa for the FEA of test F300/3, but exceeded 400 kPa for the FEA of F3700, which had almost twice the height of protective cover above the level under consideration.

9.3.1 Approximation of Soil Pressure Predicted by 3D FEA

The linear relationship between average vertical pressure above the pipe and the applied surface pressure was attractive in its simplicity, and so it was explored further to see if an approximate relationship could be developed to predict this pressure over the range of geometries and soil properties considered in the FEA of the seven field tests involving pipes placed in a trench. The linear equation can be expressed by a gradient and a y-intercept, where y is the vertical pressure 150 mm above the pipe crown averaged over the pipe diameter.

The theory of elasticity applied to the stress distribution in a homogeneous elastic half space predicts that the relative soil pressure developed under the centre of a surface pressure applied over a circular area is related to the geometry of the situation, in particular the square of the ratio of the depth to the point in the half space relative to the radius of the loaded area. So it could be expected that similar geometric factors would also be important in estimating the gradient, which is simply a load factor on the surface pressure, which provides an estimate of the average of the vertical soil pressure over the pipe radius. However the loaded soil body is neither homogeneous nor a half space, and so the breadth of the trench, the depth of layers and the relative stiffness of soil within and beside the installation could be expected to be important in estimating the average vertical pressure within the soil. If the point under consideration in the soil is underlain by less stiff soil, the pressures can be expected to be less than those predicted for a homogeneous soil mass.

The y-intercept is most likely a direct consequence of the mobilized shear stress acting on the vertical trench walls and therefore could be expected to be dependent on shear strength factors for the backfill soil and the natural soil from which the trench was formed. A simple way to express this influence is by exploring relative

stiffness of the soil (Young's moduli) rather than relative shear strength. Geometric factors such as the depth of the point below the loaded surface and the width of the trench relative to the width of the loaded area can be expected to be important. The greater the depth, the greater the likelihood of the development of the full shear capacity between the soils both in and beside the trench. Likewise, if the perimeter of the loaded surface area is closer to the trench wall, the shear strength on the trench wall would be mobilized more readily.

9.3.1.1 The y-intercept

It was found that the y-intercept varied almost linearly with the inverse of the ratio, Z/B, where B is the width of the trench and Z is the depth below the surface of the backfill to a height 150 mm above the pipe crown. The data have been plotted in Figure 9-25. A linear trendline has been imposed emanating from the origin. Inclusion of consideration of the stiffness of the backfill soil relative to the stiffness of the natural soil improved the regression coefficient from an R^2 of 0.74 to 0.846 (refer Figure 9-26). The relationship took the form:

$$\text{y-intercept} = -104\left(\frac{Z}{B}\right)\left(\frac{E_1}{E_4}\right)^{0.27} \qquad 9\text{-}2$$

where E_1 = Young's modulus of the backfill soil

E_4 = Young's modulus of the natural soil

9.3.1.2 The gradient

The first step in seeking a correlation was to review simple elasticity theory for the stress developed beneath the centre of a uniformly loaded circle resting on a homogeneous and isotropic half space. The vertical stress in this case is given by the equation:

$$\sigma_z = q\left[1 - \left(\frac{1}{\left(1 + \left(r/z\right)^2\right)}\right)^{1.5}\right]$$

or $$\sigma_z = q(LF) \qquad 9\text{-}3$$

where σ_z = additional vertical stress in the soil at depth z due to surface loading

q = uniform applied surface pressure

r = radius of the circular area

z = depth below the centre of the circle to the point at which σ_v is required

LF = load, or stress influence factor

The formula for the load factor was applied with an equivalent radius, based on a circular area equivalent to the rectangular area of the loading plate. It was found that for the data from the FEA of the field tests, a regression coefficient (or R^2) of just 0.61 was obtained for a linear correlation between the gradient and the load factor.

Geometric factors were reviewed separately for potential correlation with the gradient. The gradient was found to increase both with the square of the ratio of the width of the loading plate, b, and the depth, Z, as well as the ratio of the width of the trench, B, to the pipe diameter, D. An improved correlation ($R^2 = 0.78$) was evident when the data were plotted against the product of these geometric ratios, $(b/Z)^2(B/D)$, as shown in Figure 9-27.

A much stronger linear correlation was achieved by comparing the gradient with the product of the geometric ratios, divided by the load factor from equation 9-3. The data have been plotted in Figure 9-28 and the regression coefficient can be seen to be close to unity (0.983). The resultant equation for the gradient is:

$$\text{Gradient} = \frac{0.214\left[\left(\frac{b}{Z}\right)^2\left(\frac{B}{D}\right)\right]}{LF} - 0.085$$

or

$$\text{Gradient} = \frac{0.214\left[\left(\frac{b}{Z}\right)^2\left(\frac{B}{D}\right)\right]}{\left[1-\left(\frac{1}{\left(1+\left(r/z\right)^2\right)}\right)^{1.5}\right]} - 0.085 \qquad 9\text{-}4$$

Attempts were made to introduce relative stiffness factors such as the ratio of Young's moduli of the soil backfill and the sidefill, or surround soil (E_1:E_2). The ratio of the stiffness of the pipe ($S = EI/D^3$) to the Young's modulus of the surround soil, when incorporated into the formulation, was found to provide a small improvement in the correlation; the regression coefficient was increased by just 0.5%. The stiffness ratio was provided with an exponent, which was found to be approximately 0.1 to achieve the best correlation. The resultant expression was:

$$\text{gradient} = \frac{0.484\left(\frac{S}{E_2}\right)^{0.1}\left[\left(\frac{b}{Z}\right)^2\left(\frac{B}{D}\right)\right]}{LF} - 0.036 \qquad 9\text{-}5$$

The corresponding plot has been provided in Figure 9-29. It would seem that the Young's moduli of the soil within and beside the installation and the stiffness of the pipe are far less significant than the geometric factors, for the range of material properties and geometries considered in this investigation.

9.3.1.3 The chosen expression

The gradient and intercept of the linear relationship between the average vertical pressure 150 mm above the pipe and the applied vertical pressure were based on equations 9-2 and 9-4. The improvement afforded by equation 9-5 was considered to be relatively insignificant and not worth the added complexity of the expression. It is of interest to observe that the soil and pipe stiffness terms were of little significance in determining the average vertical stress above the pipe, for the range of values in these seven finite element analyses. However the range of moduli of the soil was limited; the ratios of E_1 to E_2 and E_1 to E_4 ranged between only 0.7 to 1.5 and 0.12 to 0.35, respectively. In addition, the stiffness of the pipe, S, was low and varied between 0.76 and 1.02 kN/m^2.

A simple bi-linear expression was adopted which set the average vertical pressure in the soil to zero if negative values of average vertical pressure above the pipe crown were determined at low levels of applied surface pressure. At higher surface pressures, the assumed linear relationship became operative. In reality, a transitional relationship could have been adopted from zero applied surface pressure until the

average pressure above the pipe became linearly related to the applied external pressure, as observed in the tests, however the simplification was felt to be inconsequential.

Examples of the fit of the adopted expression to the finite element analysis data are provided in Figure 9-30 to 9-32 for each of the pipe diameters. It is evident that the chosen expression adequately reflects the development of pressure within the backfill due to the rectangular patch load on the surface, albeit the pressure averaged across the pipe diameter. In the next section, this average vertical pressure is combined with a simple expression to estimate pipe movements with construction traffic loading.

9.3.1.4 Estimates of pipe movements of field tests based on the average vertical stress approximation from FEA

The empirical stress analysis was combined with estimates of the modulus of soil reaction of the surround soil and the various simple methods available to designers (Iowa, Watkins, Hoeg and AASHTO, as cited by Dhar et al, 2002 (refer equations 2-40 and 41)), to produce estimates of the movements of the pipes in the four field tests. The modulus of soil reaction was based on the initial soil density index of the surround (after AS/NZS2566.1-1998). No correction was made to the soil modulus for the influence of the stiffness of the adjoining clay of the trench walls.

The AASHTO method requires a vertical arching factor, which was calculated to be 1.04 for all the pipes in the study (refer equation 2-42). For the purpose of the Iowa and AASHTO flexural equation (2-40), the deflection lag factor was assumed to be one for transient loading and the bedding constant was taken as 0.1 (equivalent to a bedding angle of 90°).

Hoeg's approach requires E, ν and K, being respectively Young's modulus of the surround soil and its Poisson's ratio, and the ratio of the horizontal to the vertical stresses in the soil. A Poisson's ratio of 0.25 was assumed and Young's modulus was taken to be equal to the modulus of soil reaction, E′, divided by 1.2, in accordance with the assumption that E′ is equivalent to the bulk modulus of the soil.

No correction was made on the soil modulus for the influence of the stiffness of the adjoining clay of the trench walls.

The value of K in these estimates of pipe deflections was one third, which corresponded well with the data from the FEA. The constant K was evaluated by comparing the average lateral stress in the centre of the surround over the height of the pipe, with the average vertical stress across the pipe and at a height of 150 mm above the crown. The predicted values of K increased with surface loading, ranging between 0.27 and 0.44, with an average over all seven analyses of 0.33.

Plots comparing the estimates of pipe deflection with the observed deflections have been provided in Figures 9-33 to 9-40. The diametric pipe strains estimated from all four methods have been plotted against the average applied surface pressure. As the Hoeg and AASHTO methods provide estimates of horizontal pipe movement as well, the predictions have been plotted together in Figures 9-37 to 9-40.

Of the four methods of estimating the pipe deflections with the estimated average stress above the pipe and the modulus of soil reaction from AS/NZS2566.1-1998, Watkin's equation tended to underestimate the vertical pipe deflection and the rate of its development with external loading. In comparison, the Iowa equation provided reasonable design estimates of the vertical diametric strain of the pipe up to strains of –4 %, -1.5% and –2% for tests F300/3, F375/7 and F450/3, respectively. Both the Iowa and Watkins' equations underestimated the pipe strain for tests F450/4.

It was found that the estimates from Watkins' equation improved considerably when the pipe strain was based on the measured vertical pressure centrally above the crown of the pipe. The dashed lines in the plots for tests F375/7 and F450/3 (the only two field installations with pressure cell measurements) indicate the revised estimates ("Watkins + pc data"). It is evident also that the plots reflect the measured trends well, reinforcing the belief that the greatest difficulty for the designer is the estimation of the stress distribution within the soil due to external loading.

Estimates of vertical diametric pipe strain from Hoeg's theory were generally more conservative than the Iowa equation estimates. However, the estimates of both

vertical and horizontal diametric pipe strains reflected very well the observed trends, over a broader range of pipe deflection. Estimates for the purposes of design were reasonable to a limit of approximately –3% vertical diametric strain for most tests, but to only –2% for test F450/4.

The AASHTO predictions closely followed those of Hoeg, which was not unexpected as the AASHTO approach applies similar principles. Interestingly, the two predictions were matched for all practical purposes, when the vertical arching factor was applied to the crown pressure in determining the flexural pipe movements. The difference in load assumed reaching the pipe in the two elements of pipe deformation, that is flexural and hoop compression movement, was suggested to be a failing of the approach in Chapter 2.

9.4 SUMMARY OF THE CHAPTER

In this Chapter, work from the previous Chapters was investigated in an attempt to produce simple guidelines for pipe designers, without resort to finite element analysis. As it was conceded that the non-paved laboratory soil box tests were not an adequate reflection of field conditions, due to the difficulty with the partial sidewall restraint, this Chapter has concentrated upon the four field tests and the corresponding FEA. Some additional FEA were made to broaden the geometric range of the installations that were modelled.

In the simple methods of estimating pipe movements (e.g. Iowa and Watkins' equations), the designer must first determine the vertical pressure above the pipe crown, which is assumed to be uniform. For a non-paved and trafficked backfill surface, this may prove to be a very difficult exercise. It has been shown that the vertical stress below the centre of a loaded rectangular area is under-predicted by the theory of elasticity (Holl, 1940), the underestimation becoming more serious with increased magnitudes of loading and plate settlement. Moreover, the stress distribution revealed by FEA was non-uniform, with stress concentrated closer to the pipe crown.

Inspection of the FEA of the field tests revealed that the average vertical stress above the pipe across a distance equal to the diameter of the pipe, was directly proportional to the average applied surface pressure. A relatively simple empirical expression has been derived subsequently between the two pressures. The expression simply requires the geometry of the installation and the ratio of the Young's modulus of the backfill soil to the Young's modulus of the natural soil forming the trench walls.

Once the "uniform" stress above the pipe is known, the designer must assign a value of the modulus of soil reaction, E′, to the surround soil. In this Chapter, values of the modulus of soil reaction, E′, were backcalculated by examining the lateral soil pressures (pressure cell data) and the deflections of the pipes as loading progressed. Using the estimates of density index of the soil based on dynamic penetration tests after preparation of each test installation, the backcalculated values were compared with recommendations of Australian Standard AS/NZS2566.1-1998. The recommended values of E′, although conservative when compared to data reported by Moore (2001), seemed to be adequate for poorly graded sand and in the correct range for design purposes.

The connection between "the modulus of soil reaction" and the Young's modulus of the sand was explored by re-analysing the plate drum tests as a loading test on an isotropic, homogeneous elastic medium. The Young's modulus for an assumed Poisson's ratio of 0.25 averaged 6.25 MPa. It was found that this value was approximately 30% lower than the value recommended by AS/NZS2566.1-1998, if the modulus of soil reaction, E′, was assumed equivalent to the constrained or bulk modulus, M, as proposed by Watkins (1988) and adopted by AASHTO. The relationship between E, a measurable soil property, and E′ should be explored further.

Watkins' hypothesis that "the vertical soil strain" should be equal to or greater than the vertical diametric strain of the pipe was generally verified. Calculation of the soil strain was based on the measured pressure above the pipe crown and the experimental values of the surround modulus of soil reaction, corrected for the location of the pressure cell opposite the pipe springline. Based on these data, the

450 mm diameter pipes could be expected to have contributed the least resistance to deflection of all the pipes tested.

Finally a review of flexible pipe design approaches was undertaken in conjunction with the approximation of the average vertical stress above the pipe, based on the FEA. The moduli of soil reaction adopted in these estimates were in accordance with AS/NZS2566.1-1998. Young's modulus, which is required in Hoeg's approach, was based on the previously discussed assumption of equivalence between E′ and bulk modulus.

From the limited data of the field tests, it was found that good design estimates of vertical pipe deflection could be made with the Iowa equation over the early stages of external loading. The Watkins' equation consistently produced lower estimates than the Iowa formula. Hoeg's theory and the current AASHTO approach to buried pipe design produced similar estimates, which were a little more conservative than the estimates from the Iowa equation. However deformation trends were generally well predicted, both vertically and horizontally.

The problem for the pipe designer still remains how to predict the pressure above the pipe reliably, without recourse to sophisticated FEA. A preliminary method has been suggested in this Chapter, which requires further verification.

.

9.5 REFERENCE TO THE CHAPTER

Holl, D.L. (1940). Stress transmission in earths. Proc., Highway Research Board, V20, pp 709-721. As cited by *Poulos, H. G. and Davis, E. H. (973). Elastic solutions for soil and rock mechanics. Wiley, NY.*

TABLE 9-I. Elastic soil properties of sidefill, back-calculated from pressure cell data and Hoeg's theory (1968)

Test	Profile	Height of Cover (mm)	E (MPa)	ν	K	E′ (MPa)
300/4	90VX	450	20	0.25	0.33	24
300/5	90VX	650	19	0.33	0.5	28
300/6	90VX	800	9.5	0.25	0.33	11
300/7	110VX	650	20	0.25	0.33	24
300/8	110VX	650	25	0.25	0.33	29
F375/7	110VX	700	45	0.25	0.33	54
375/8	110VX	700	15	0.25	0.33	18
F450/3	125VX	600	44	0.17	0.2	47
450/1 or 2	125VX	450	20	0.17	0.2	21

TABLE 9-II. Average vertical pressure predicted by the FEA of the field tests above the pipe crown at 40 mm surface displacement

Test	Average Vertical Soil Pressure (kPa)	
	150 mm above the crown	Level of first Gauss point (mm)
F300/3	456	406
F375/7	259	197
F450/3	247	247
F450/4	223	198

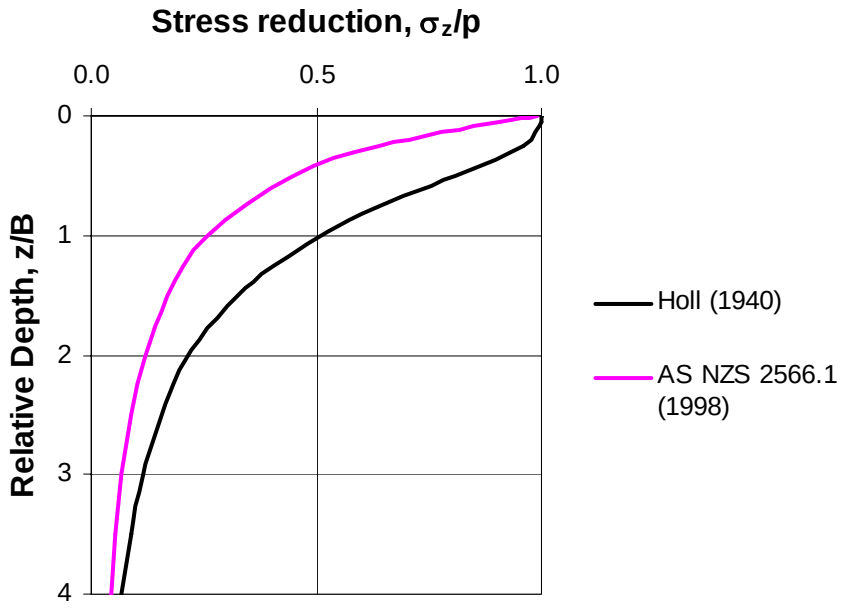

Figure 9-1. Comparison of load spreading between AS/NZS 2566.1 (1998) and theoretical elastic stress distribution

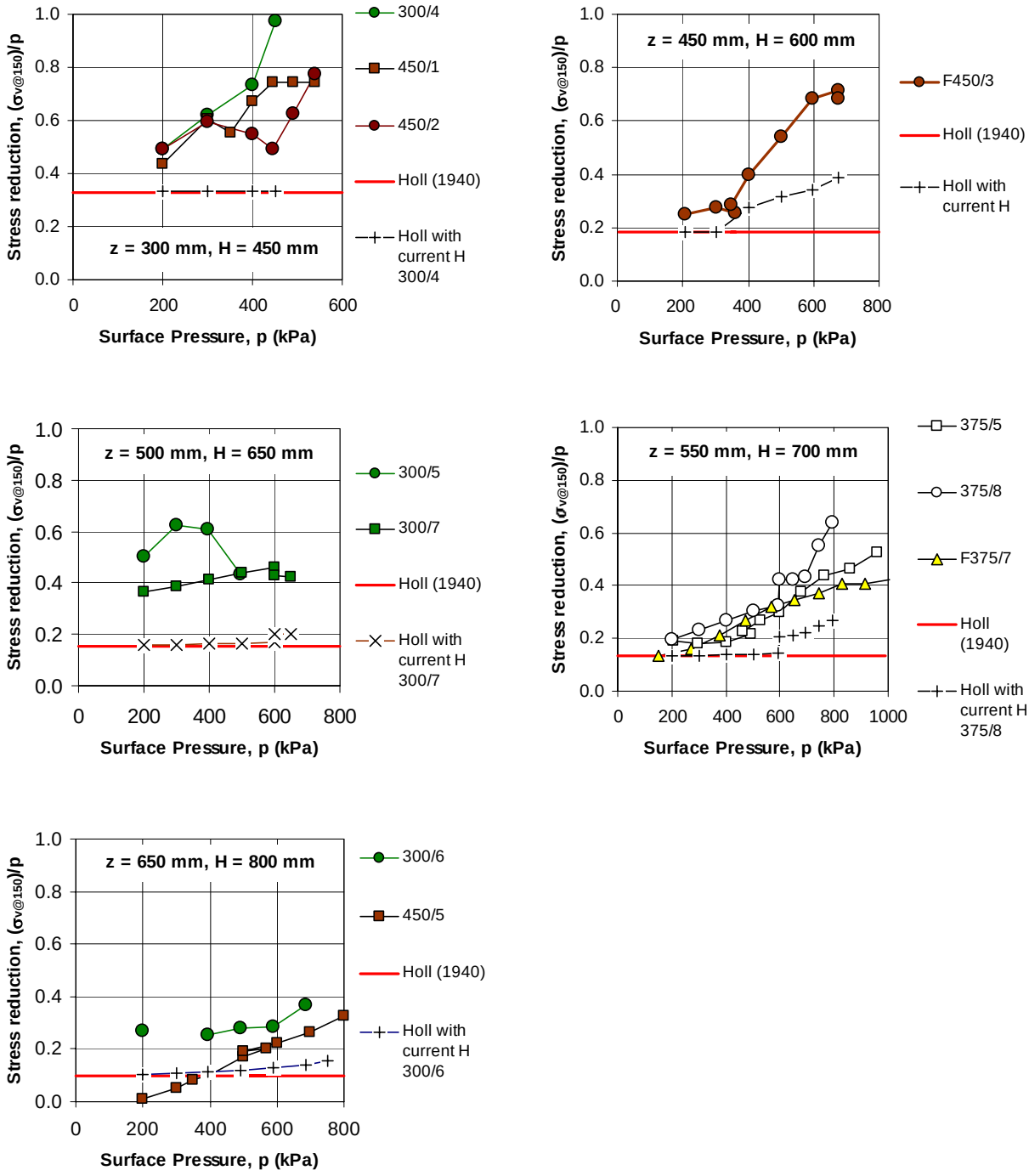

Figure 9-2. Vertical stress reduction data against applied surface pressure for various levels of backfill cover height

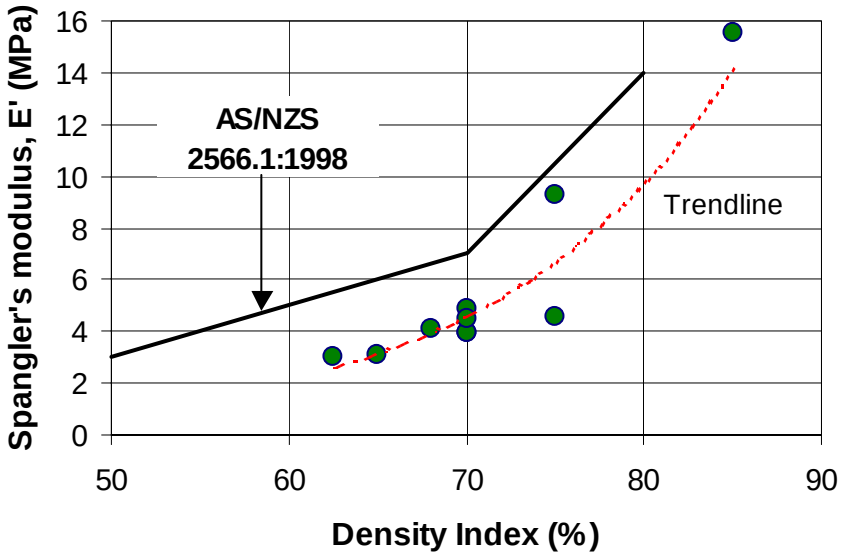

a) Uncorrected for distance between cell and springline

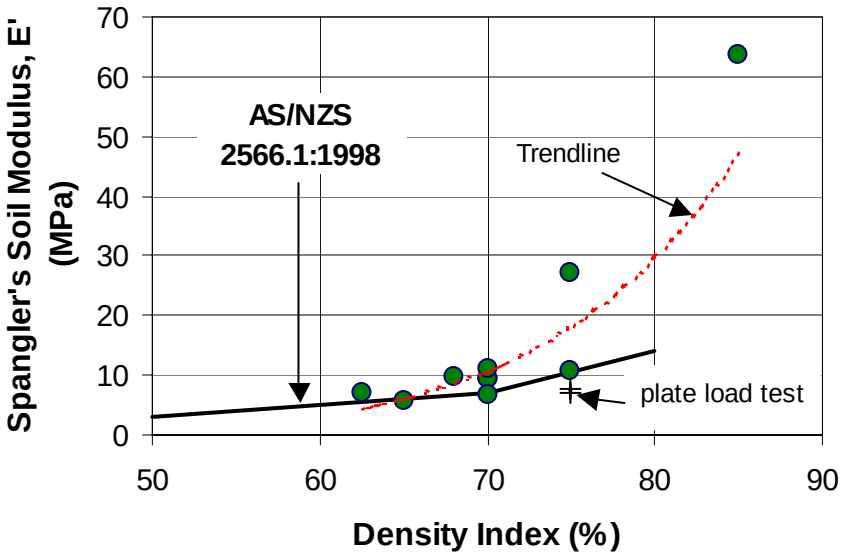

b) Corrected for distance between cell and springline

Figure 9-3. The variation of back-calculated values of the modulus of soil reaction, E′, with density index

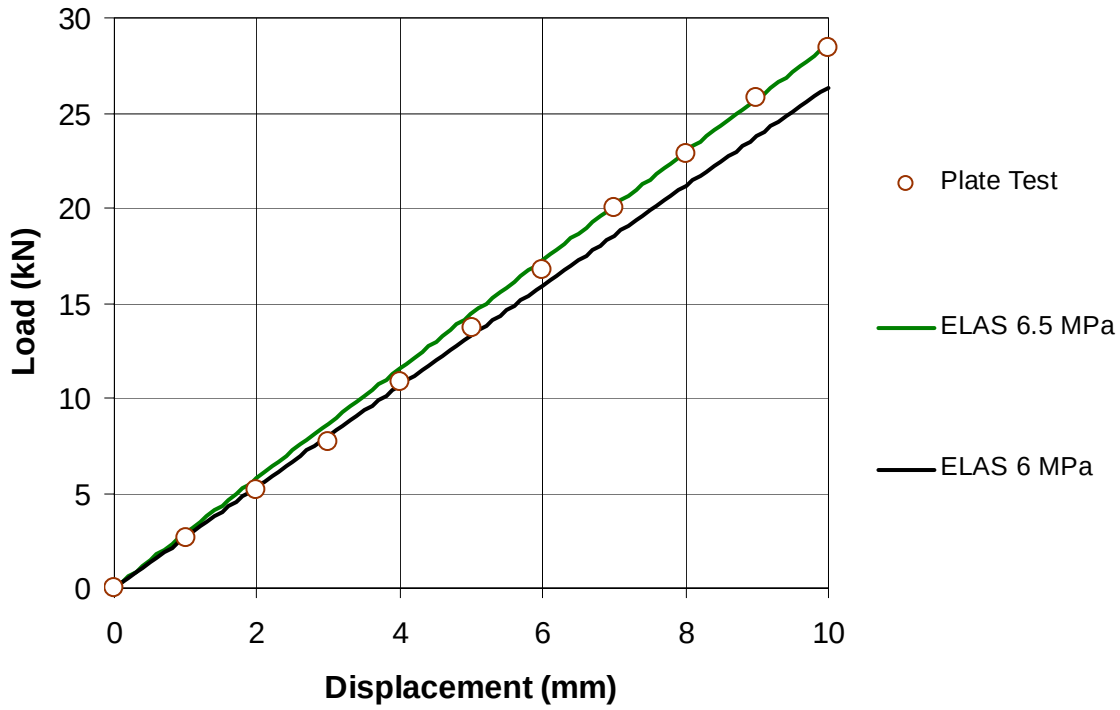

Figure 9-4. Comparison with test data and FEA of plate loading test with elastic soil, having constant Young's modulus

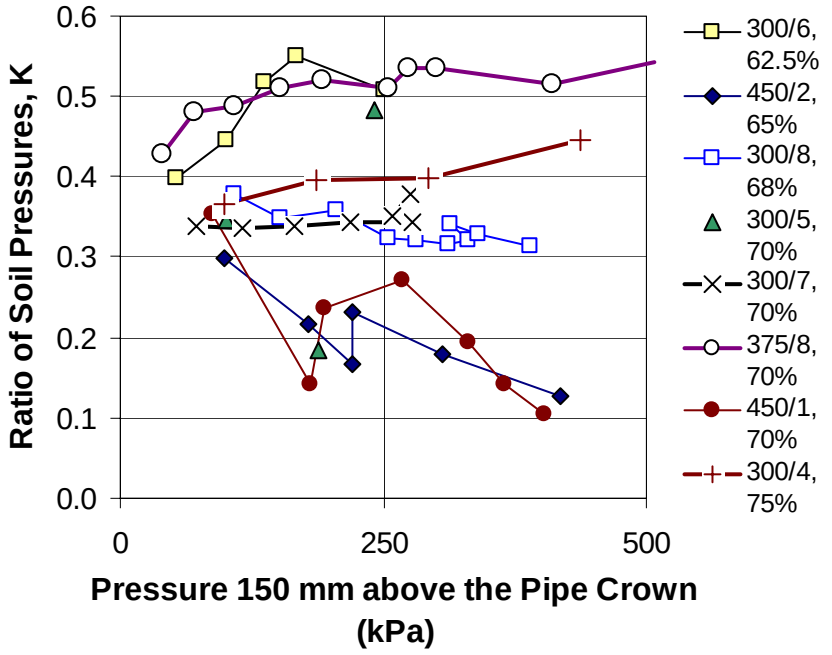

a) Laboratory soil box tests

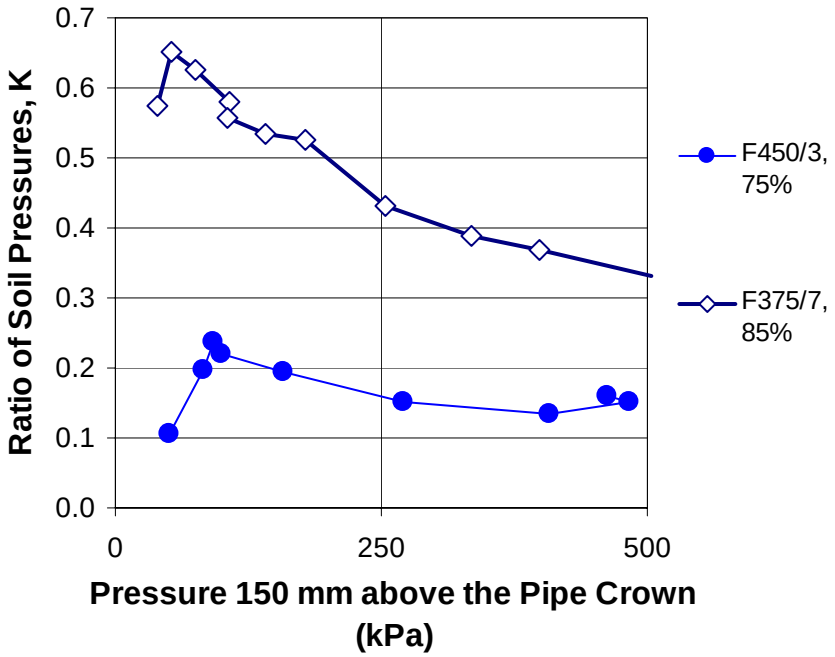

b) Field tests

Figure 9-5. Development with loading of ratios of measured soil pressures, horizontal pressure in the surround, to the vertical pressure 150 mm above the pipe crown

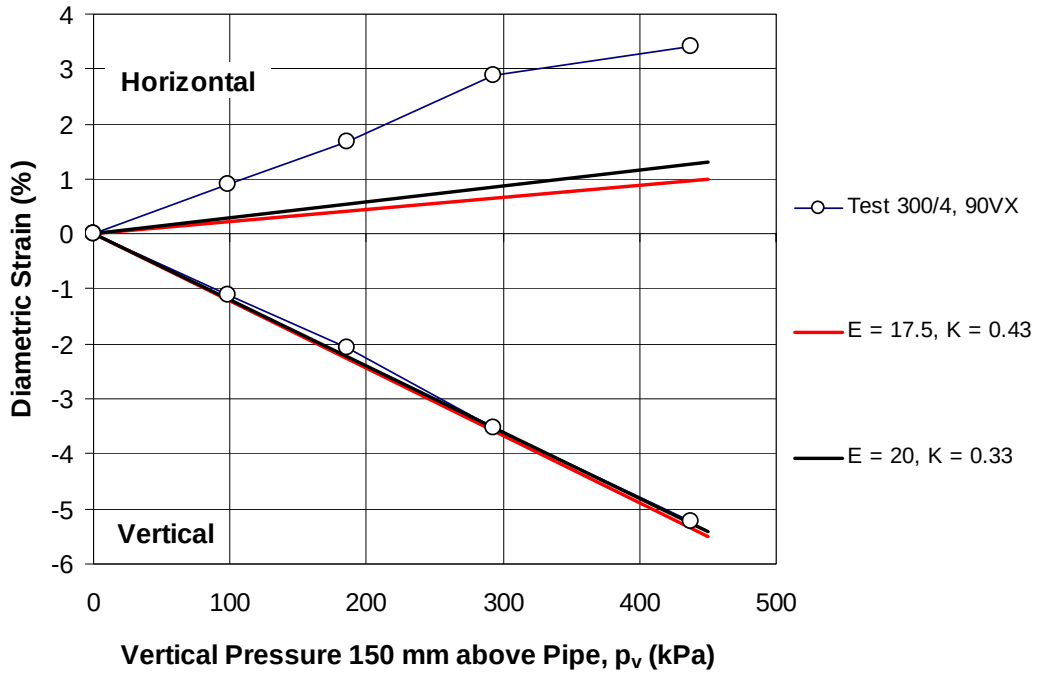

a) Test 300/4

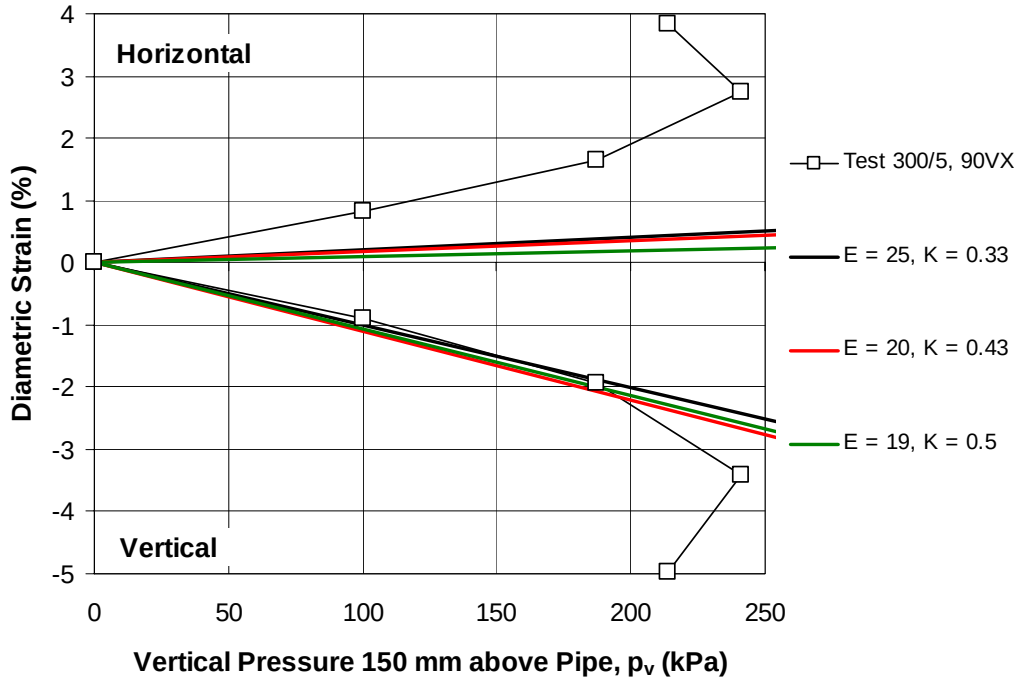

b) Test 300/5

Figure 9-6. Estimates of displacements of 300 mm diameter, 90VX pipe with 450 mm of cover, based on Hoeg (1968), assuming a perfectly rough pipe

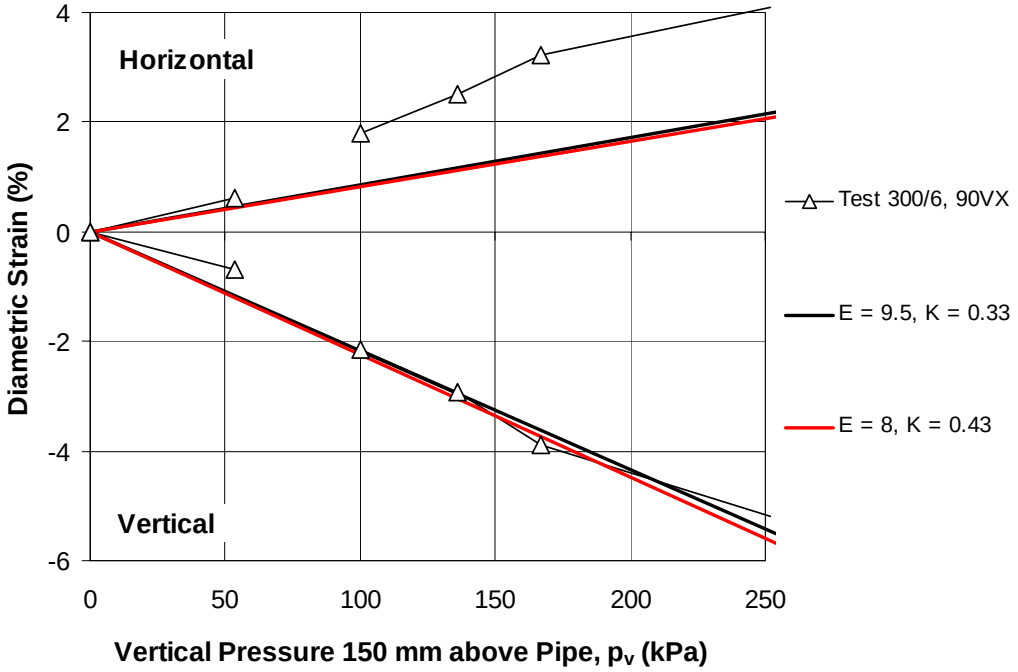

Figure 9-7. Estimates of displacements of 300 mm diameter, 90VX pipe with 800 mm of cover, based on Hoeg (1968), assuming a perfectly rough pipe

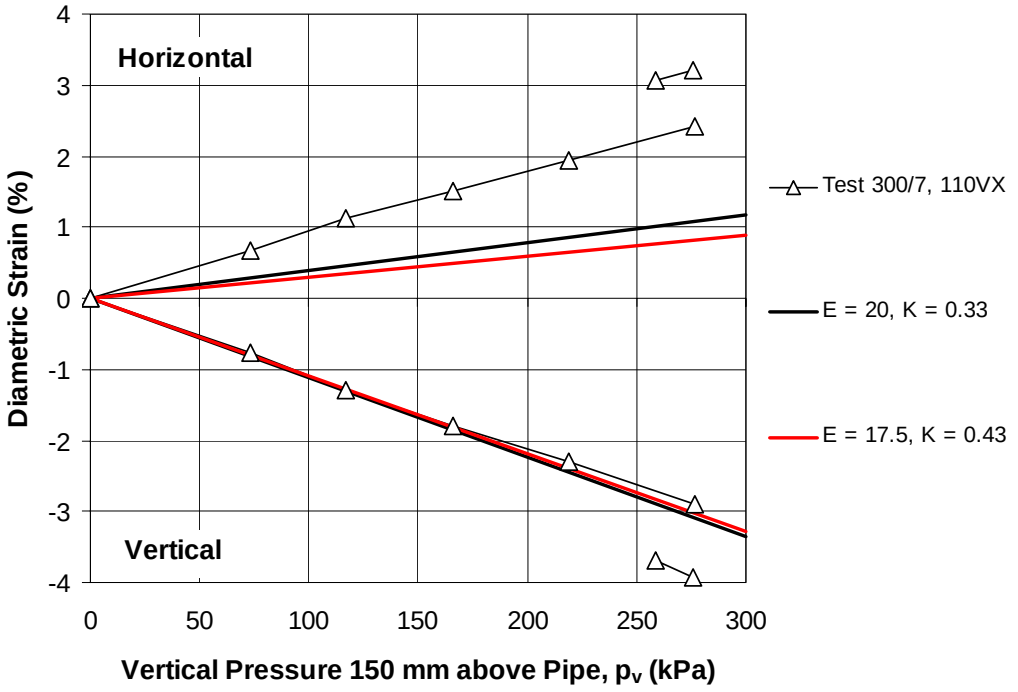

a) Test 300/7, 650 mm of cover

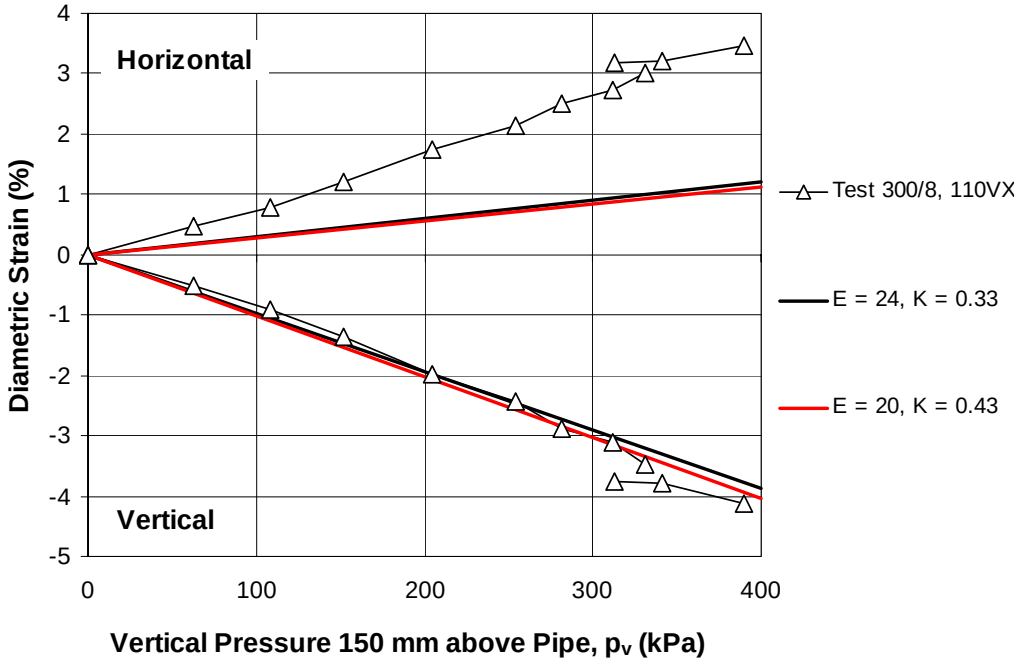

b) Test 300/8, 650 mm of cover

Figure 9-8. Estimates of displacements of 300 mm diameter, 90VX pipe with 450 mm of cover, based on Hoeg (1968), assuming a perfectly rough pipe

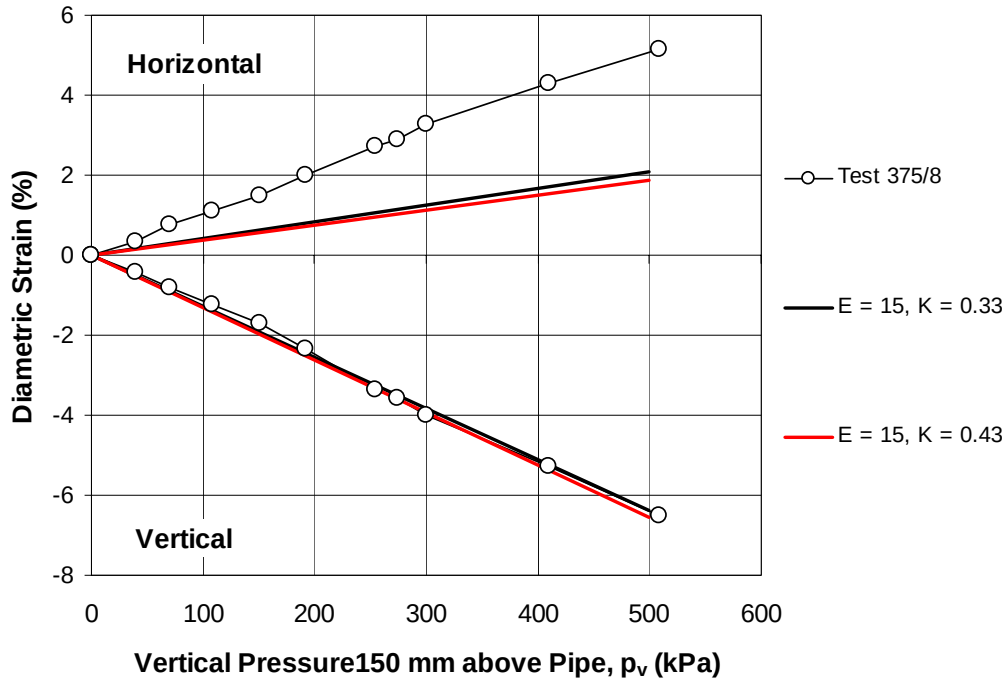

a) Test 375/8, 700 mm of cover

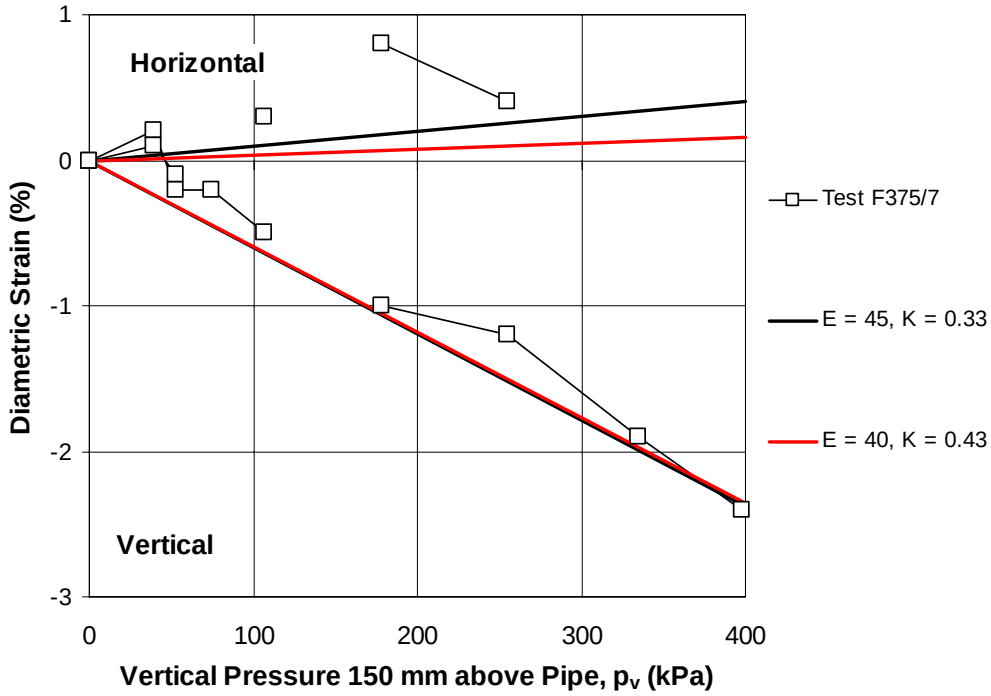

b) Field test F375/7, 700 mm of cover

Figure 9-9. Estimates of displacements of 375 mm diameter pipe based on Hoeg (1968), assuming a perfectly rough pipe

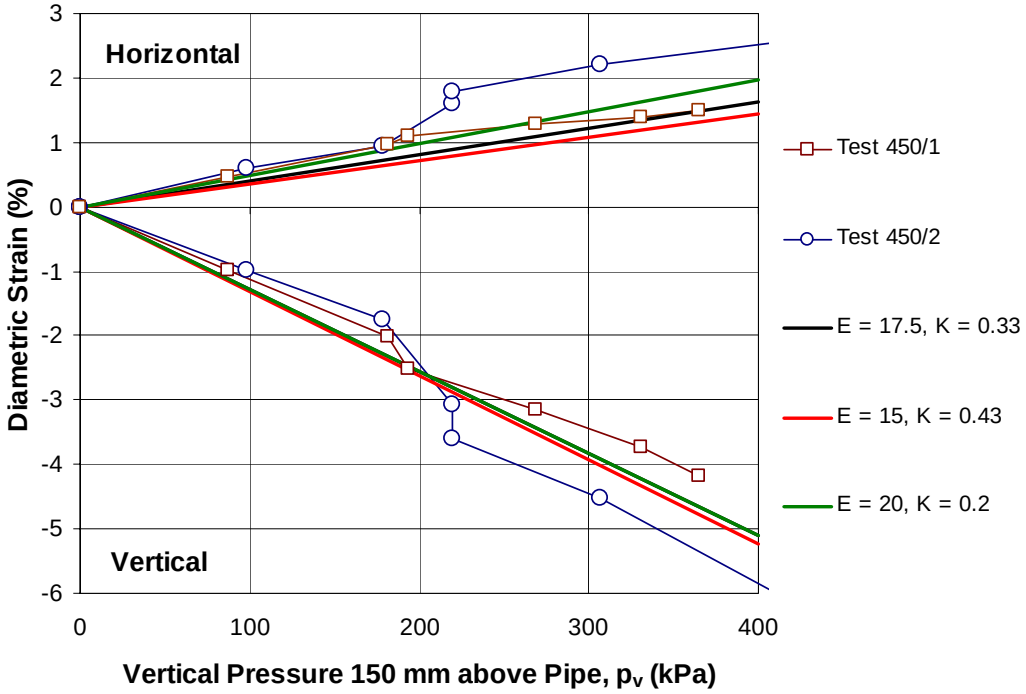

a) Tests 450/1 and 450/2, 450 mm of cover

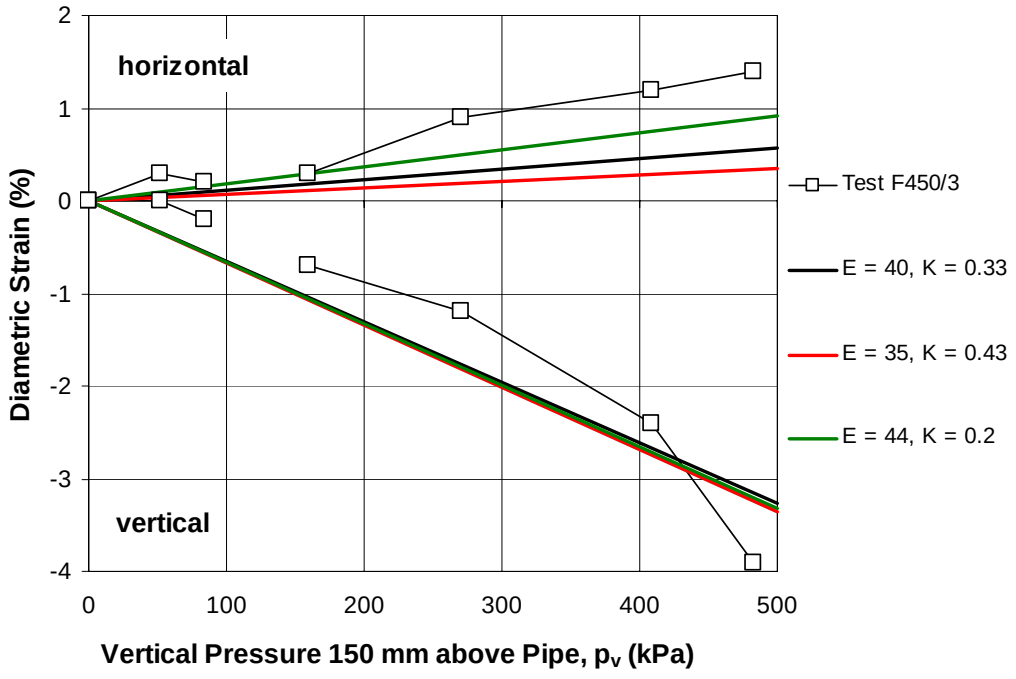

b) Field test F450/, 700 mm of cover

Figure 9-10. Estimates of displacements of 450 mm diameter pipe based on Hoeg (1968), assuming a perfectly rough pipe

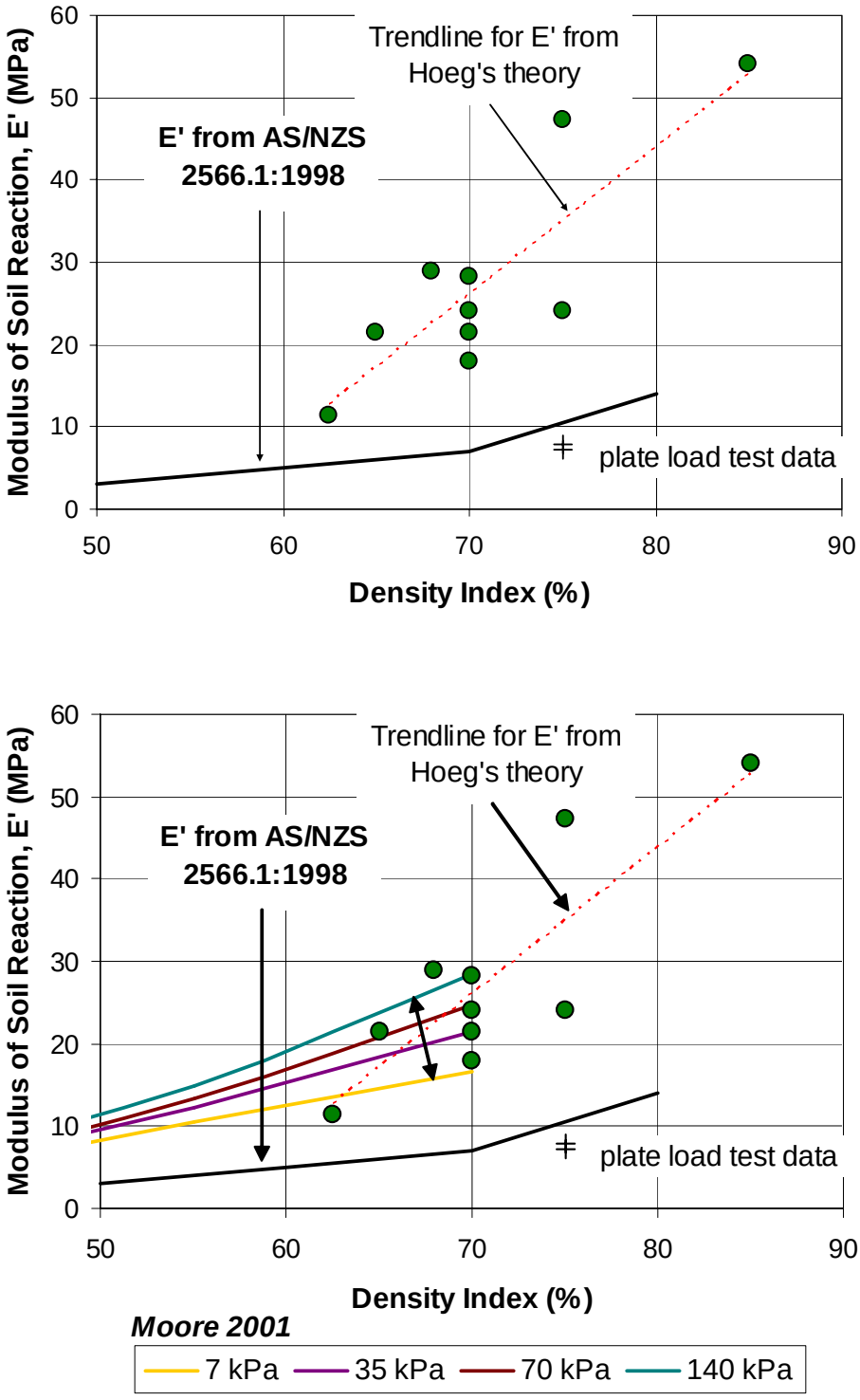

Figure 9-11. The variation of back-calculated values of the modulus of soil reaction, E′, with density index, based on Hoeg's theory (1968)

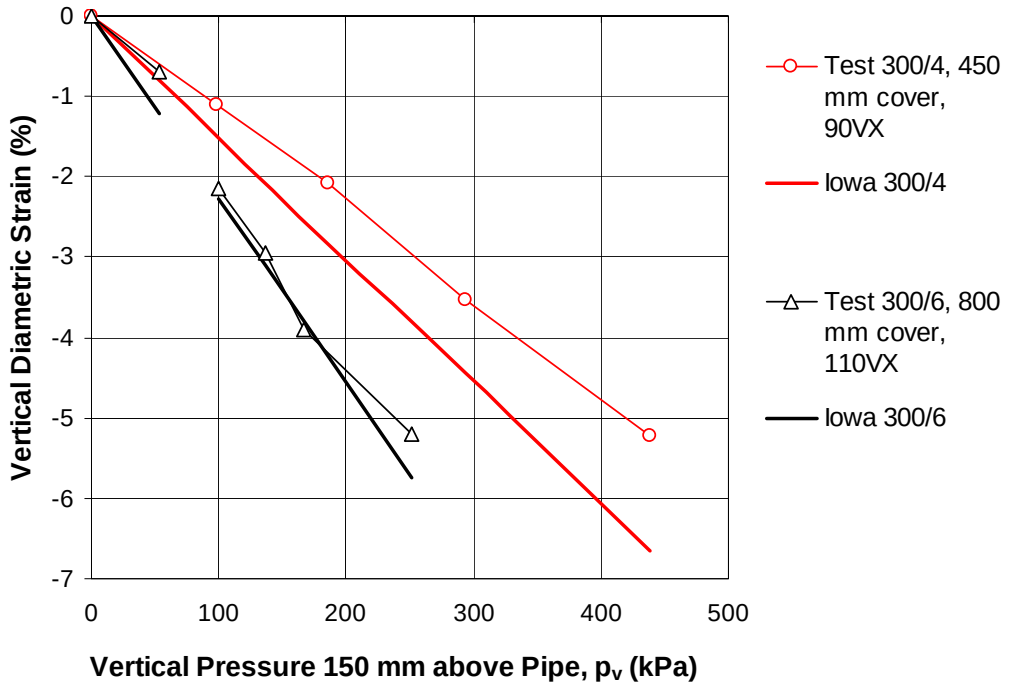

a) 90VX, 450 mm cover (Test 300/4) and 110VX, 800 mm cover (Tests 300/6)

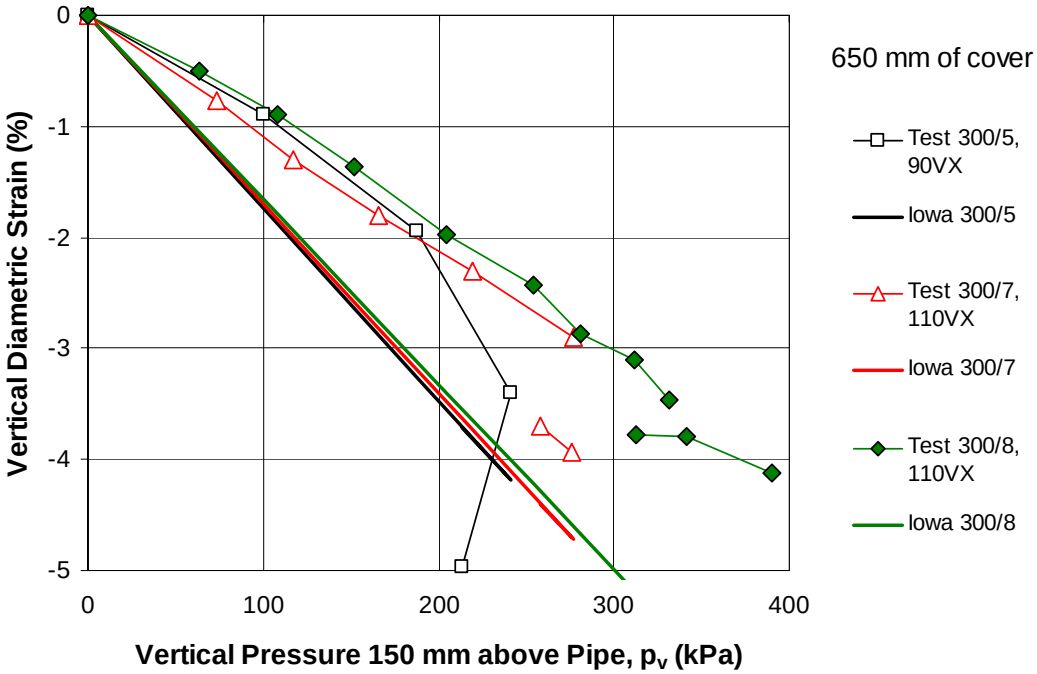

b) 90VX and 110VX with 650 mm of cover

Figure 9-12. Vertical pipe deflection estimates based on the Iowa formula and back-calculated values of E′ (300 mm diameter pipes)

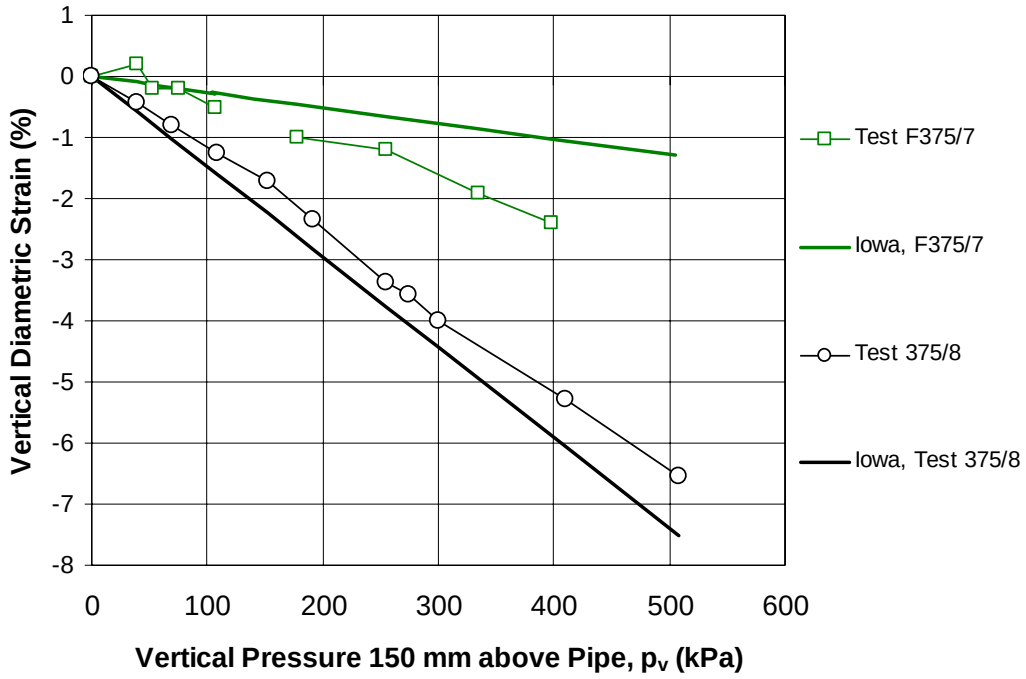

Figure 9-13. Vertical pipe deflection estimates based on the Iowa formula and back-calculated values of E′ (375 mm diameter pipes)

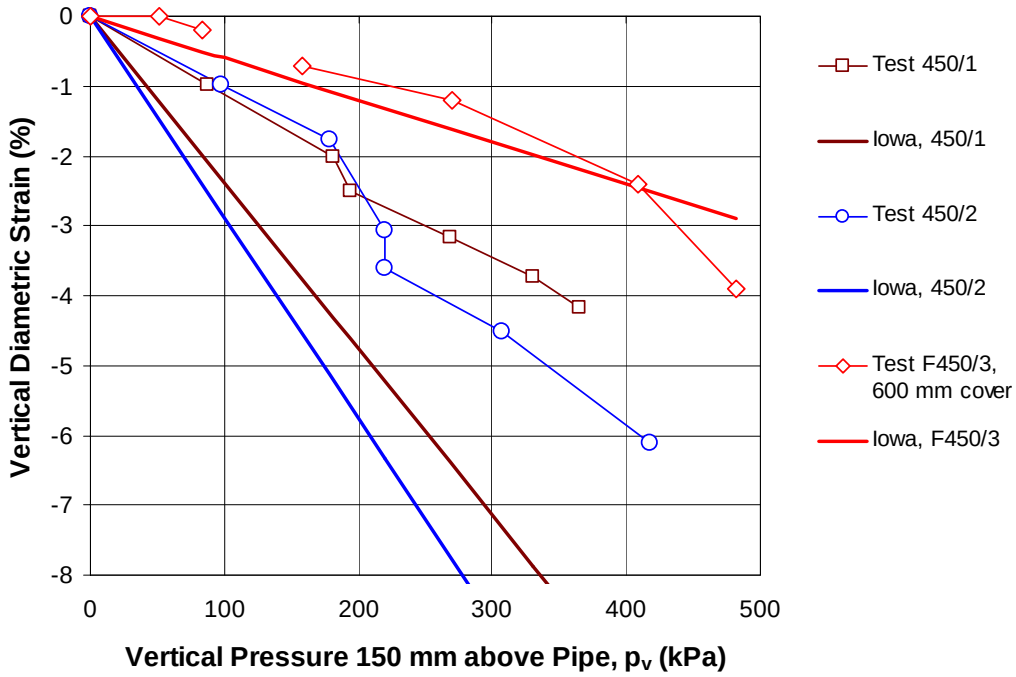

Figure 9-14. Vertical pipe deflection estimates based on the Iowa formula and back-calculated values of E′ (450 mm diameter pipes)

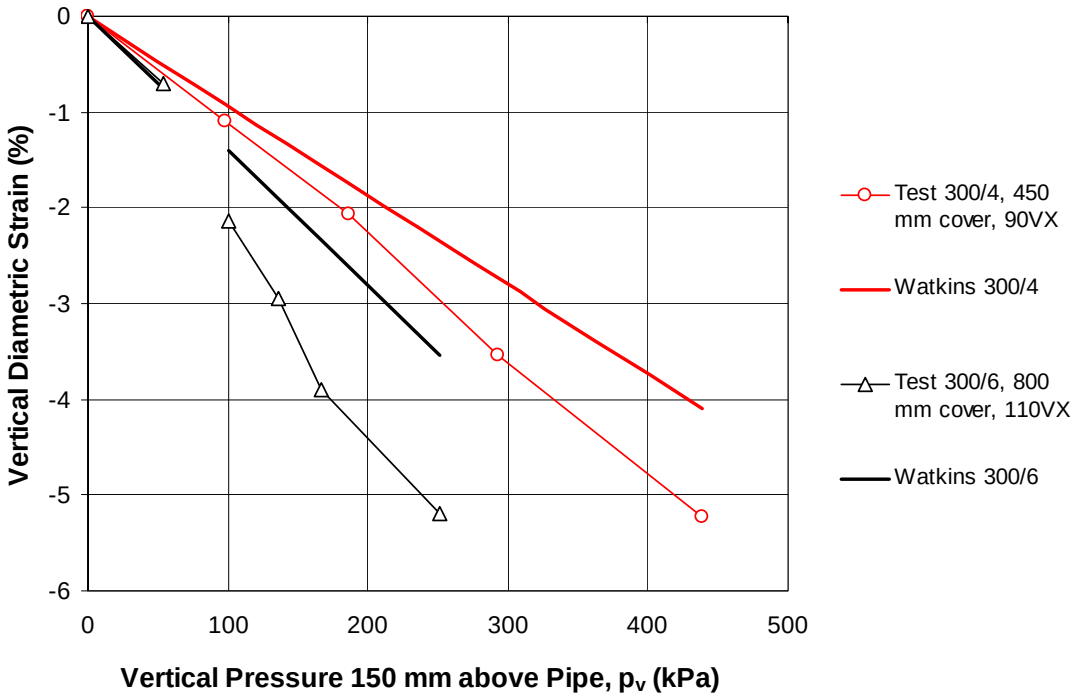

a) 90VX, 450 mm cover (Test 300/4) and 110VX, 800 mm cover (Tests 300/6)

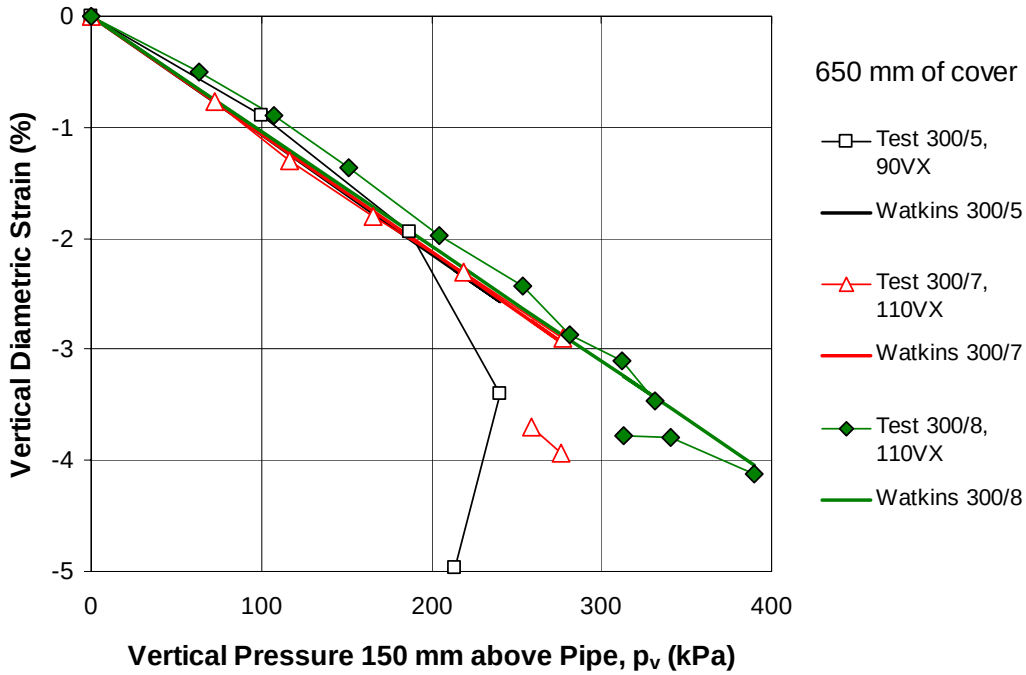

b) 90VX and 110VX with 650 mm of cover

Figure 9-15. Vertical pipe deflection estimates based on Watkins' formula and back-calculated values of E′ (300 mm diameter pipes)

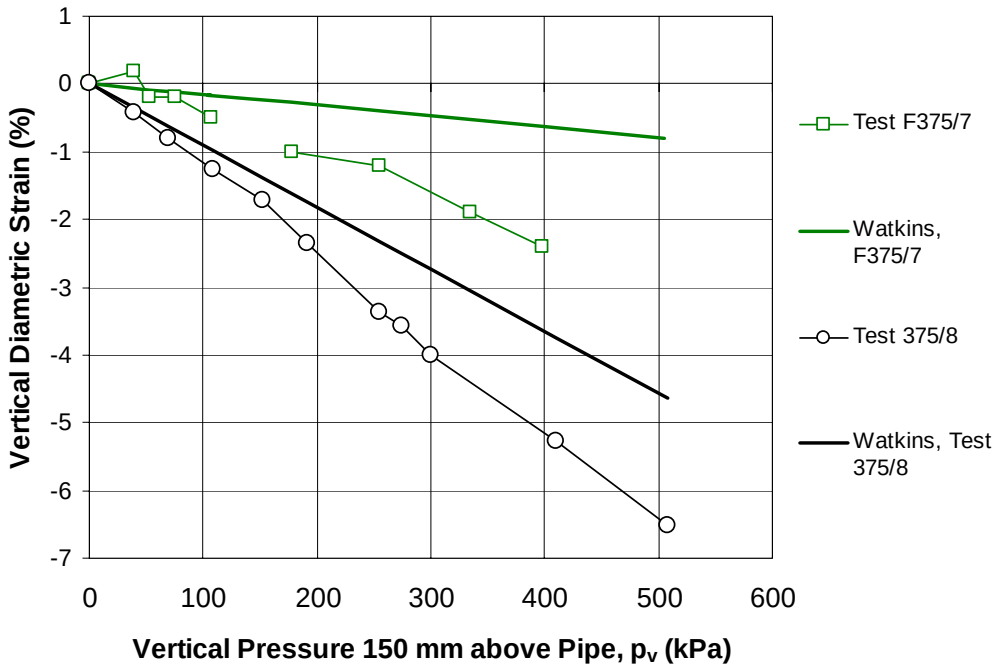

Figure 9-16. Vertical pipe deflection estimates based on Watkins' formula and back-calculated values of E′ (375 mm diameter pipes)

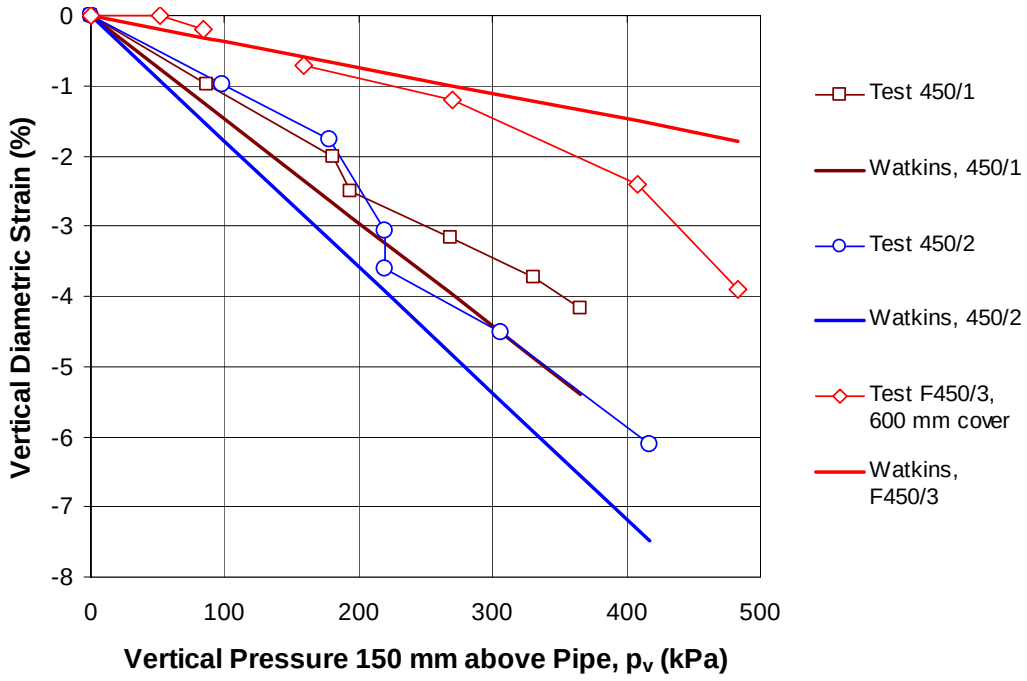

Figure 9-17. Vertical pipe deflection estimates based on Watkins' formula and back-calculated values of E′ (450 mm diameter pipes)

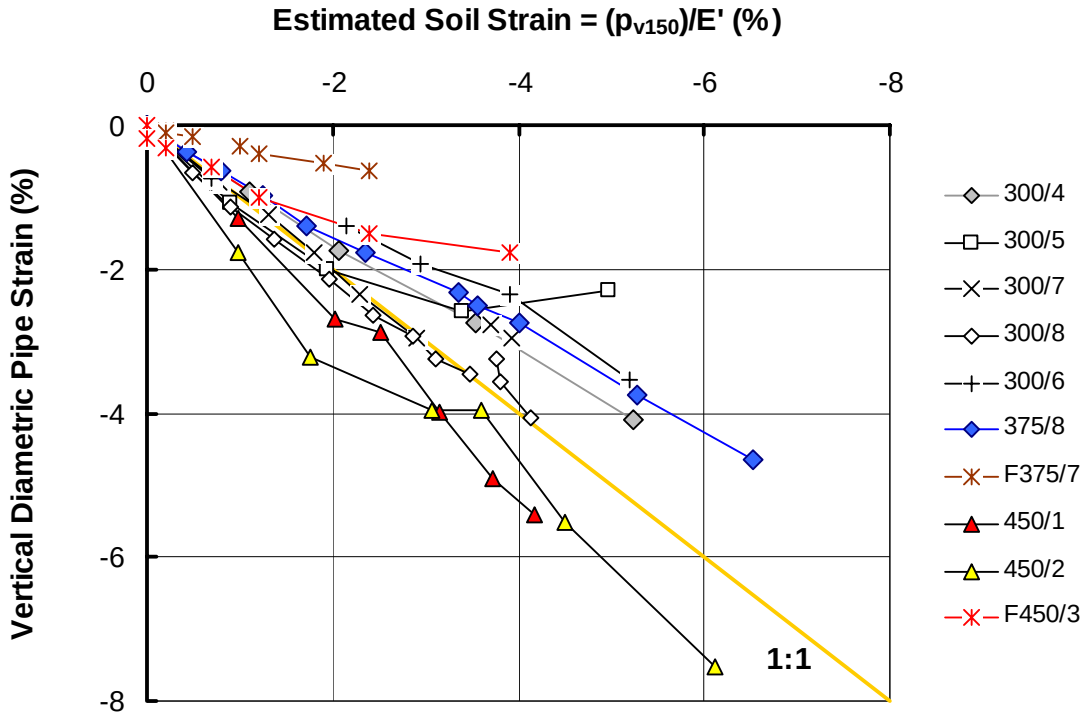

Figure 9-18. Soil strain against vertical diametric pipe strain for pipe tests with pressure cell measurements; E′ from Figure 9-3b

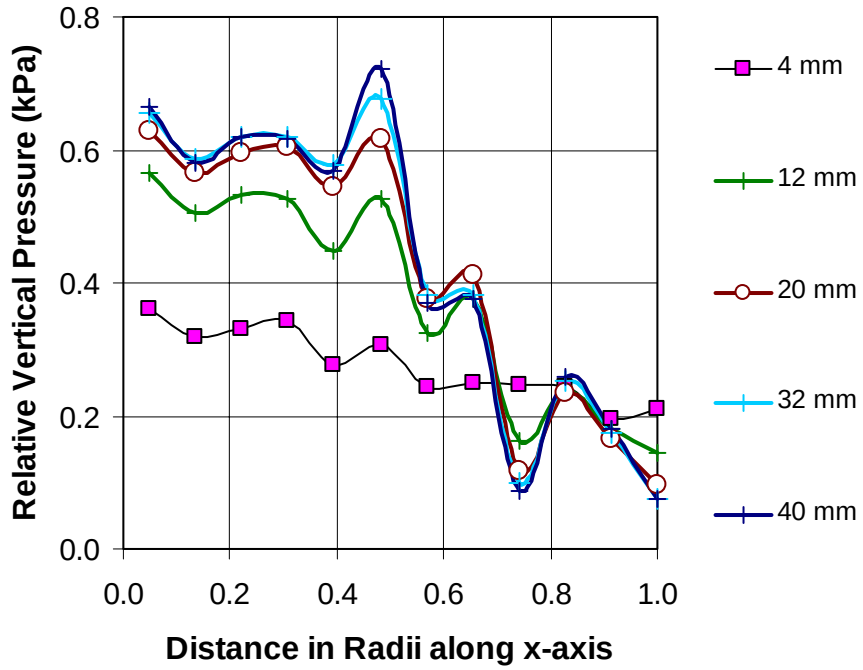

a) Vertical pressure 150 mm above the crown

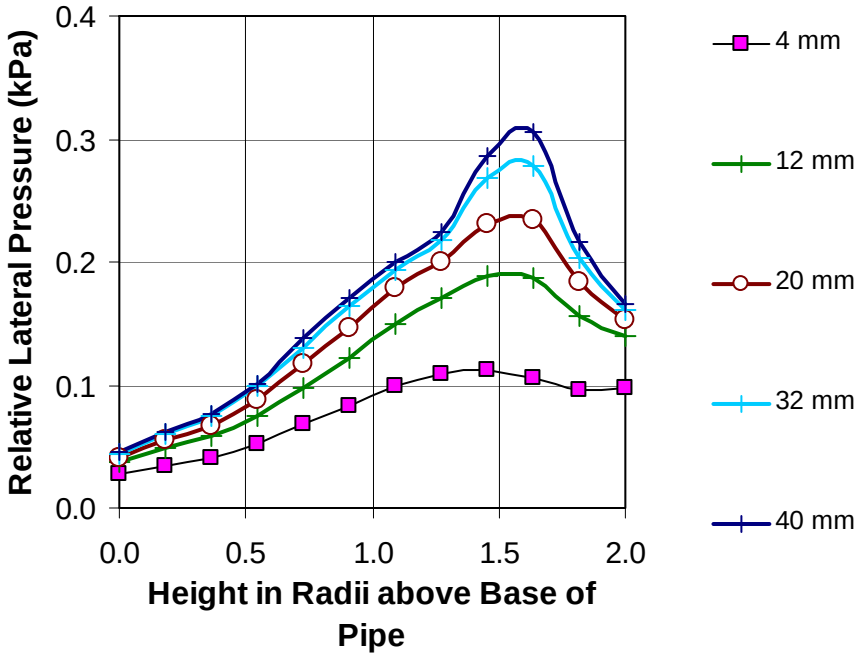

b) Lateral pressure within the surround

Figure 9-19. Soil pressure distributions predicted by FEA for F300/3 as surface plate displacements (refer legend) proceeded

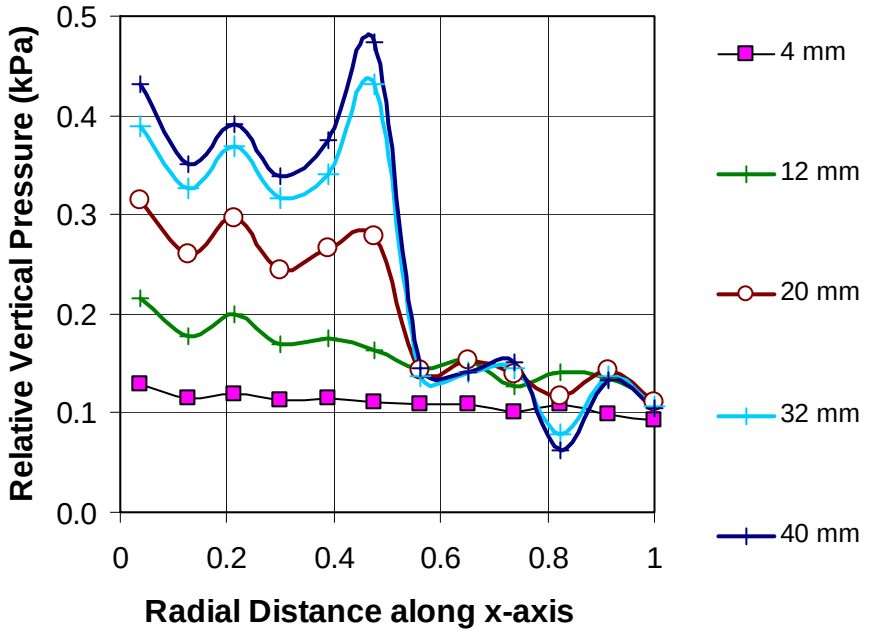

a) Vertical pressure 150 mm above the crown

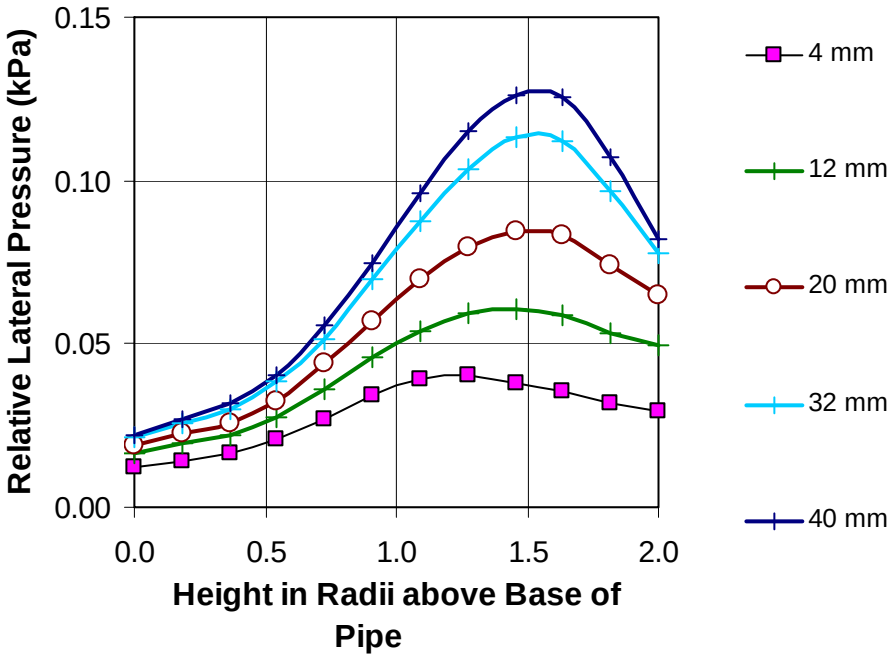

b) Lateral pressure within the surround

Figure 9-20. Soil pressure distributions predicted by FEA for F375/7 as surface plate displacements (refer legend) proceeded

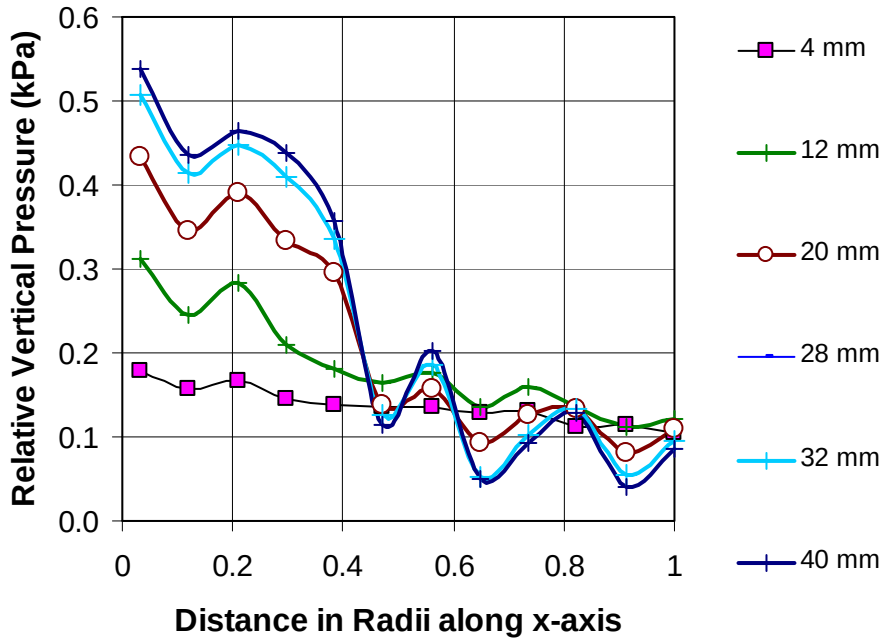

a) Vertical pressure 150 mm above the crown

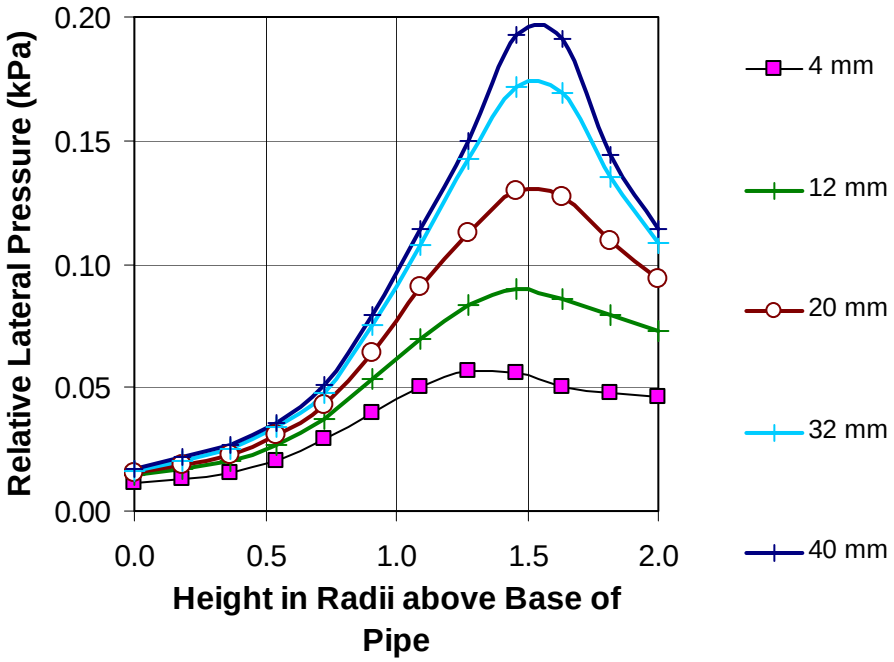

b) Lateral pressure within the surround

Figure 9-21. Soil pressure distributions predicted by FEA for F450/3 as surface plate displacements (refer legend) proceeded

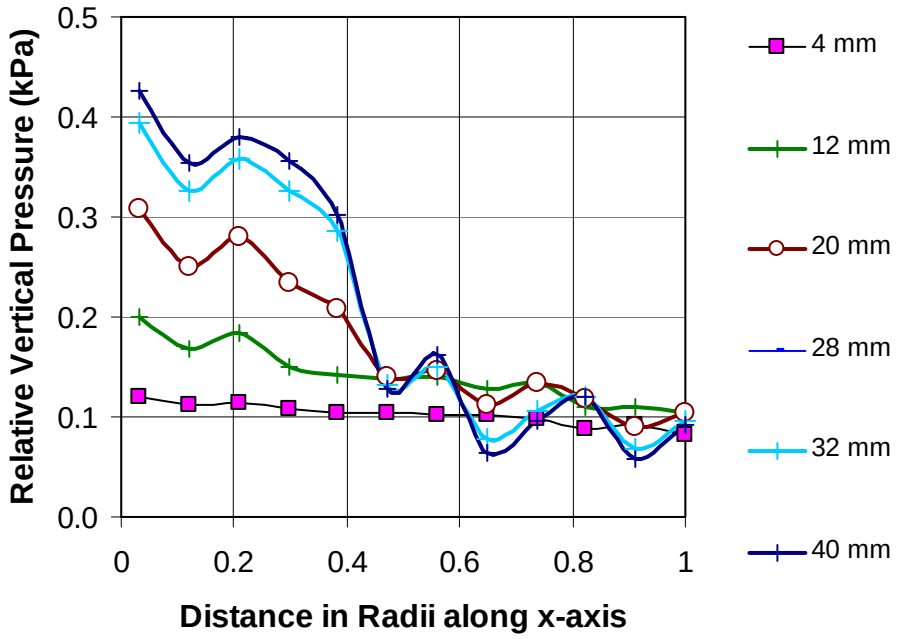

a) Vertical pressure 150 mm above the crown

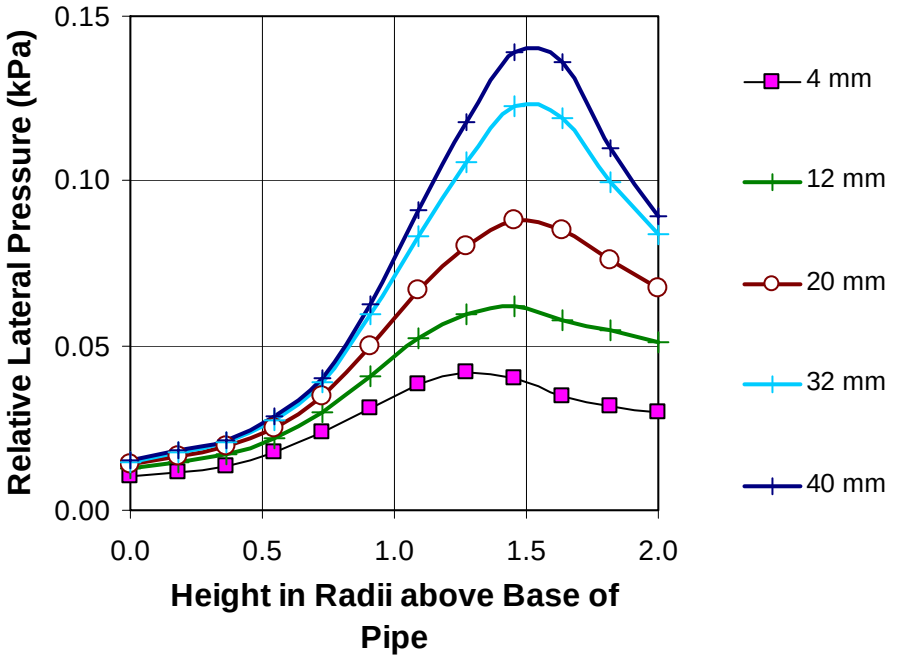

b) Lateral pressure within the surround

Figure 9-22. Soil pressure distributions predicted by FEA for F450/4 as surface plate displacements (refer legend) proceeded

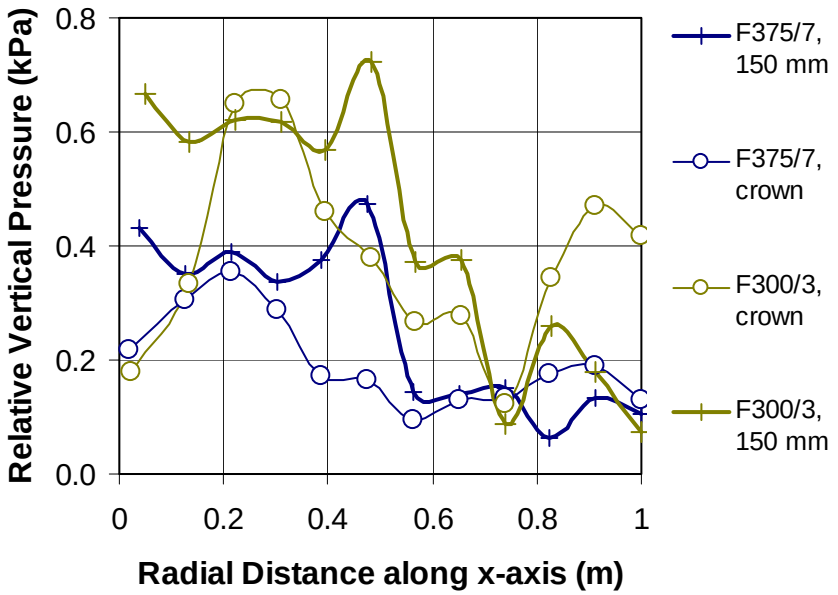

Figure 9-23. Predicted vertical soil pressure distributions above the pipe for tests F300/3 and F375/7 after 40 mm of plate displacement

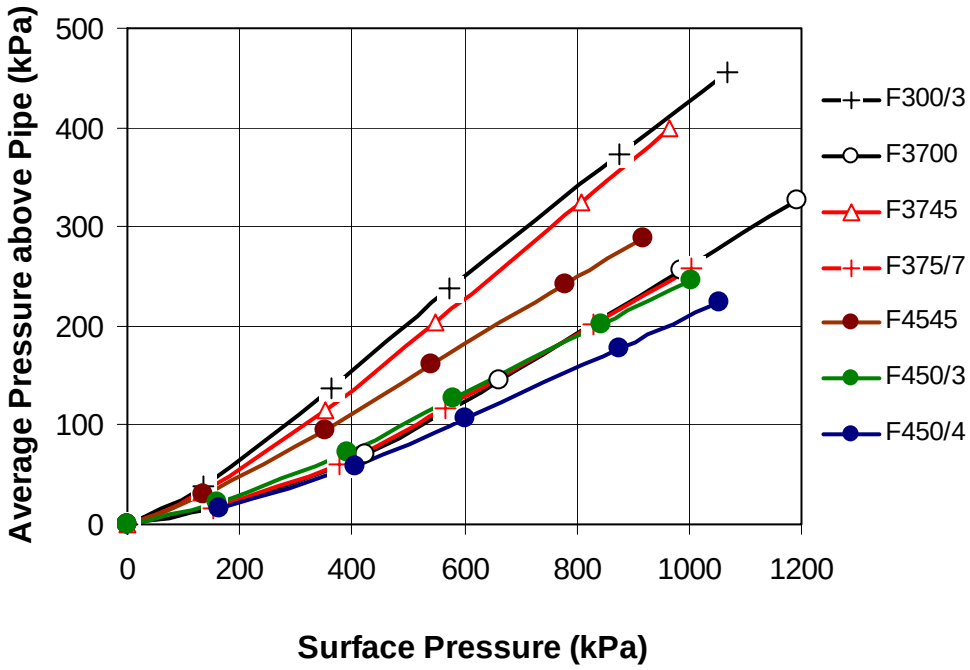

Figure 9-24. Predicted (FEA) average vertical pressure 150 mm above the pipe against the average applied surface pressure

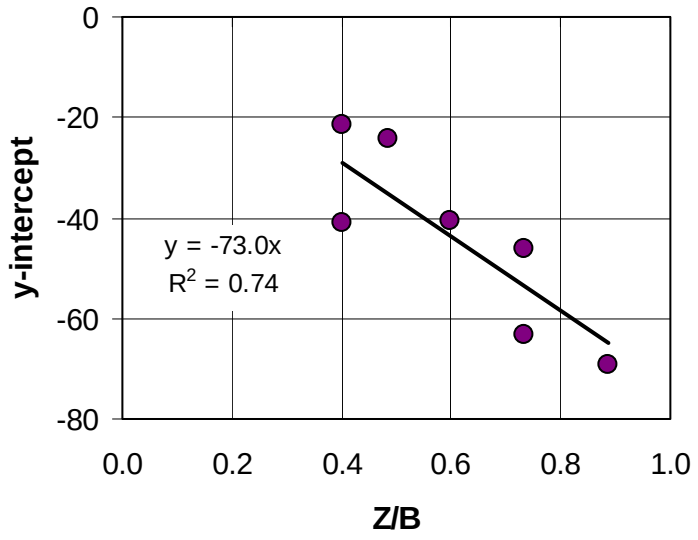

Figure 9-25. Intercept parameter for estimation of average vertical soil pressure above the pipe as a function of geometry (Z = depth to point above pipe; B = breadth of trench)

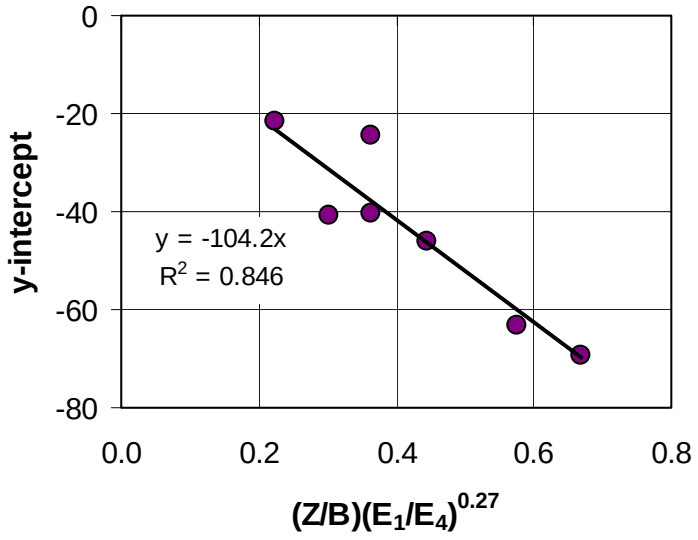

Figure 9-26. Intercept parameter for estimation of average vertical soil pressure above the pipe as a function of geometry and relative soil stiffness (E_1 = Young's modulus of backfill; E_4 = Young's modulus of natural soil)

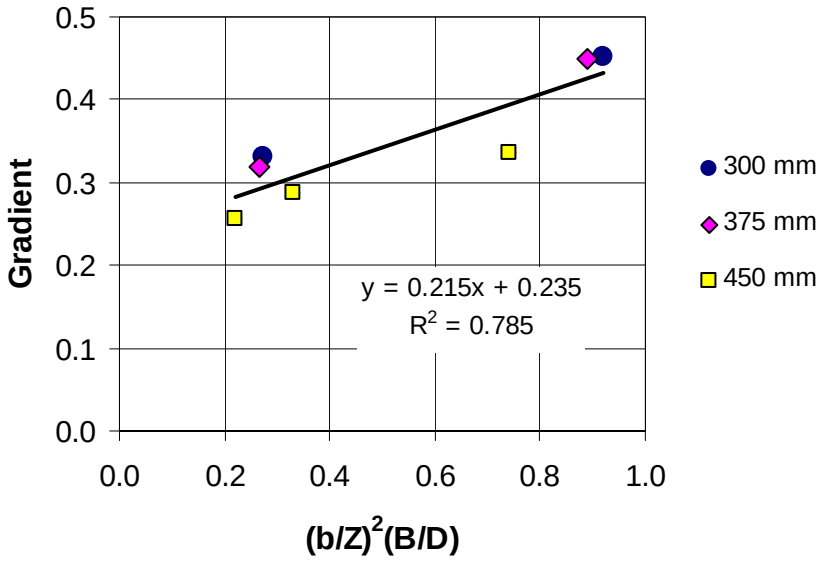

Figure 9-27. Gradient parameter for estimation of average vertical soil pressure above the pipe as a function of geometry (b = breadth of loading plate; D = pipe diameter)

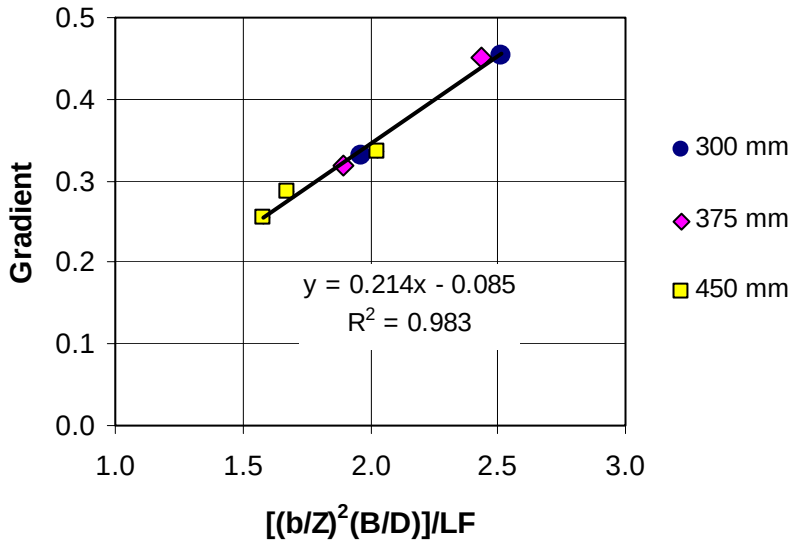

Figure 9-28. Gradient parameter for estimation of average vertical soil pressure above the pipe as a function of geometry and load factor from the theory of elasticity for a uniformly load circle

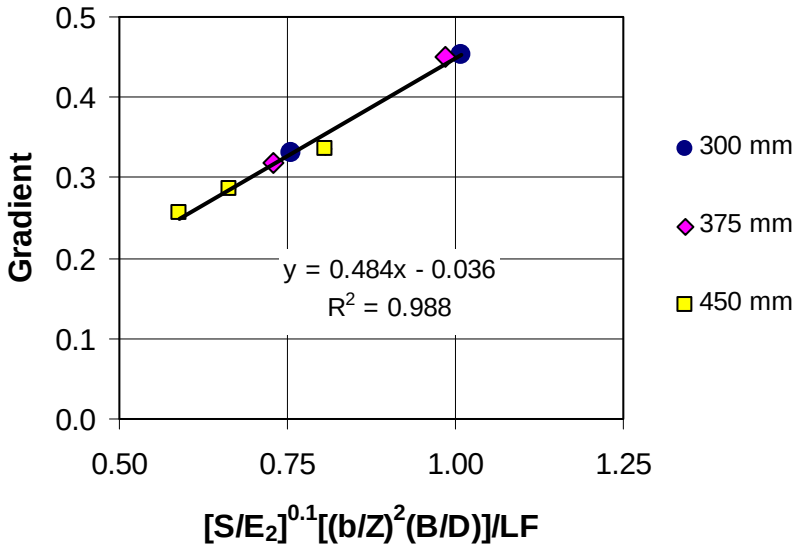

Figure 9-29. Gradient parameter for estimation of average vertical soil pressure above the pipe as a function of geometry, load factor from the theory of elasticity and stiffness factors (S = stiffness of pipe; E_2 = Young's modulus of surround)

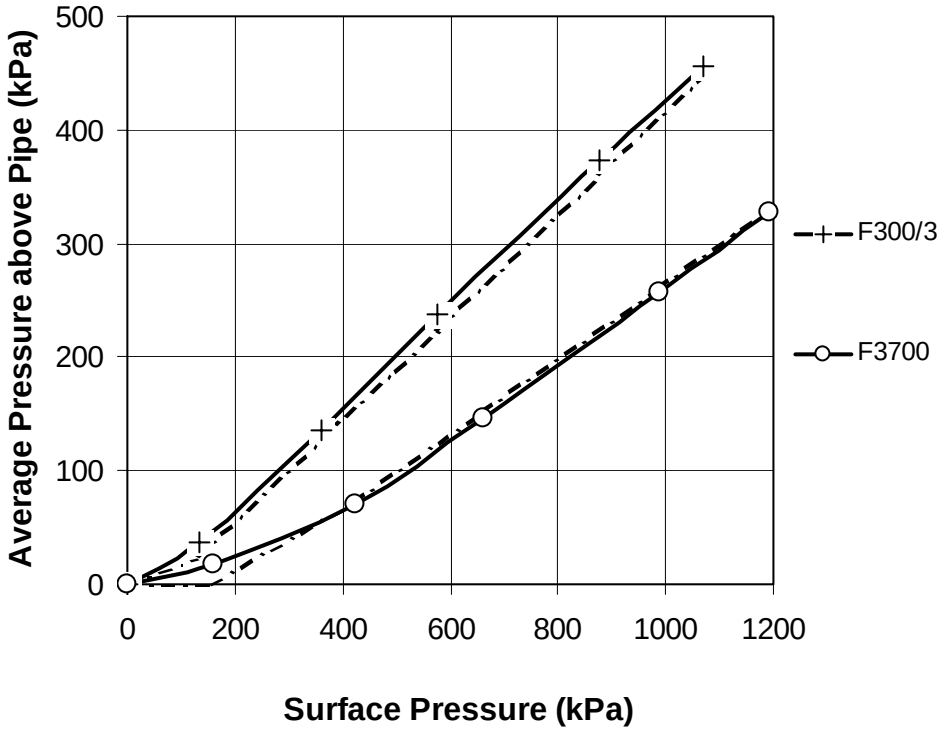

Figure 9-30. Empirical pressure relationship compared with experimental data for 300 mm diameter pipes (dashed line = empirical data)

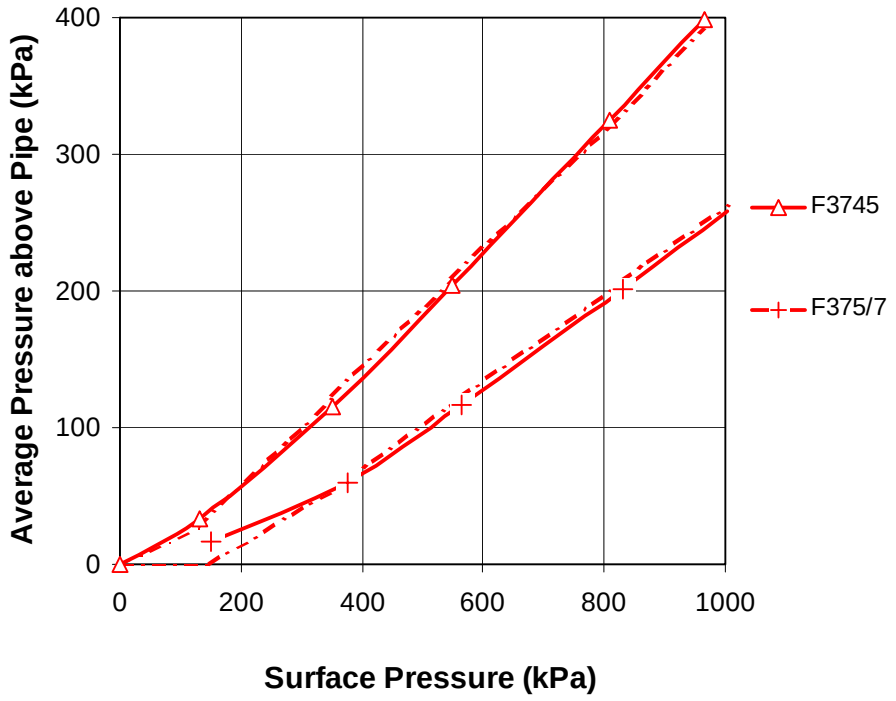

Figure 9-31. Empirical pressure relationship compared with experimental data for 375 mm diameter pipes (dashed line = empirical data)

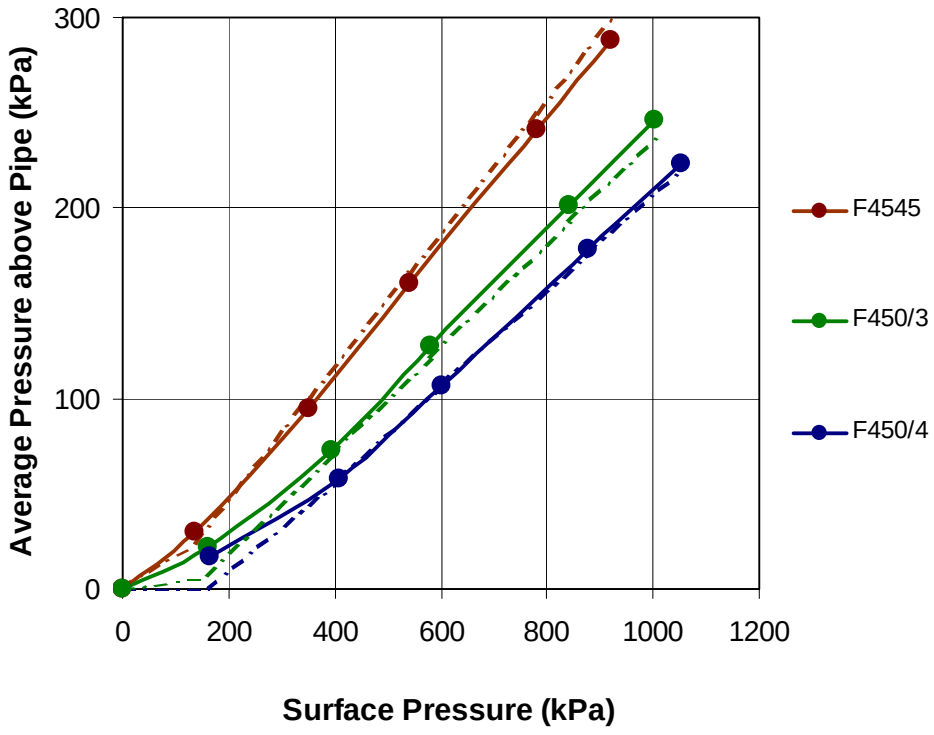

Figure 9-32. Empirical pressure relationship compared with experimental data for 450 mm diameter pipes (dashed line = empirical data)

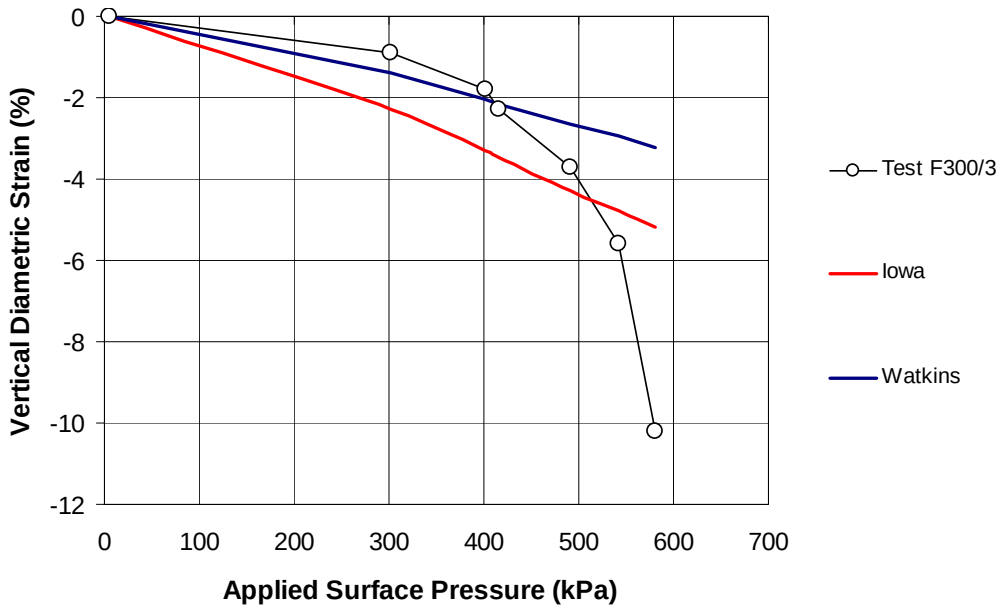

Figure 9-33. Vertical pipe deflection estimates for field test, F300/3,based on the Iowa and Watkins' formulae and the estimated average vertical pressure above the pipe

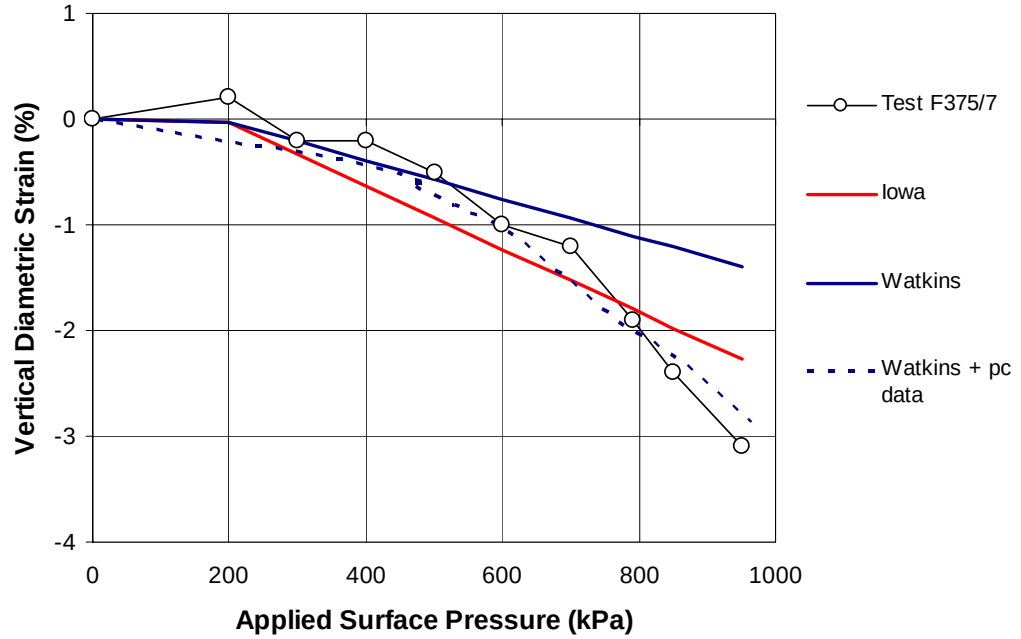

Figure 9-34. Vertical pipe deflection estimates for field test, F375/7,based on the Iowa and Watkins' formulae and the estimated average vertical pressure above the pipe

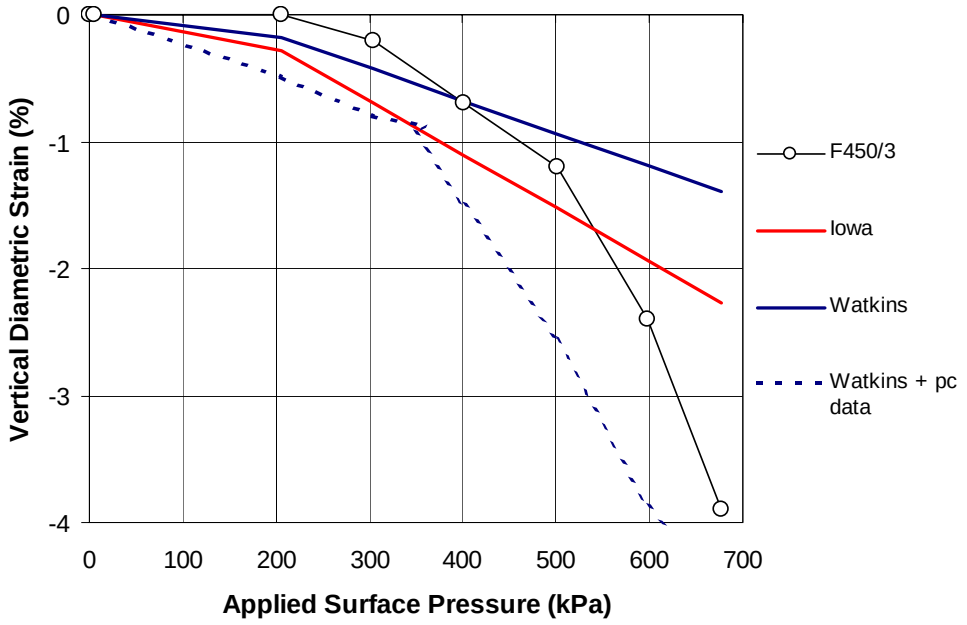

Figure 9-35. Vertical pipe deflection estimates for field test, F450/3 based on the Iowa and Watkins' formulae and the estimated average vertical pressure above the pipe

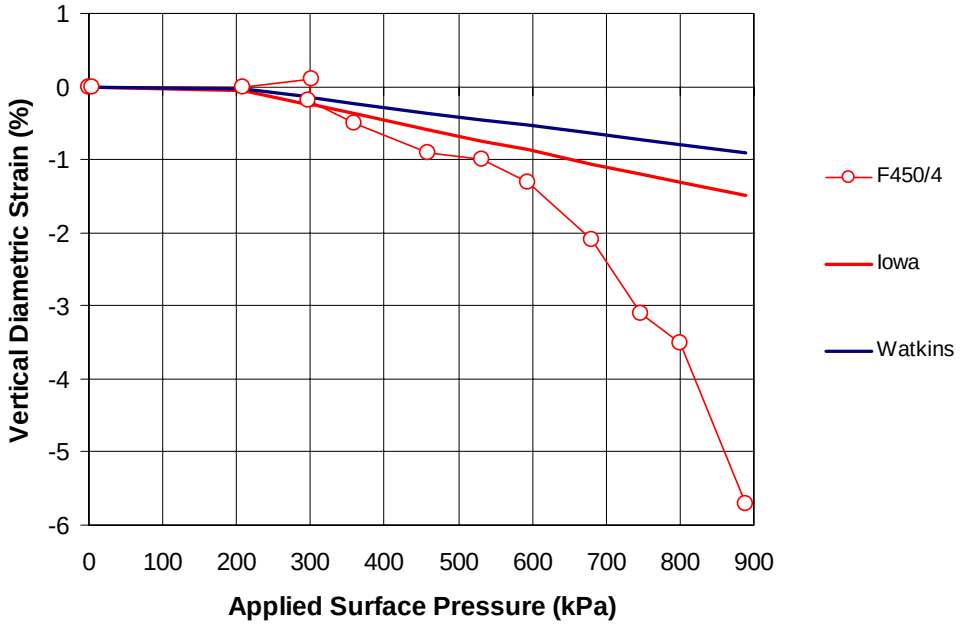

Figure 9-36. Vertical pipe deflection estimates for field test, F450/4, based on the Iowa and Watkins' formulae and the estimated average vertical pressure above the pipe

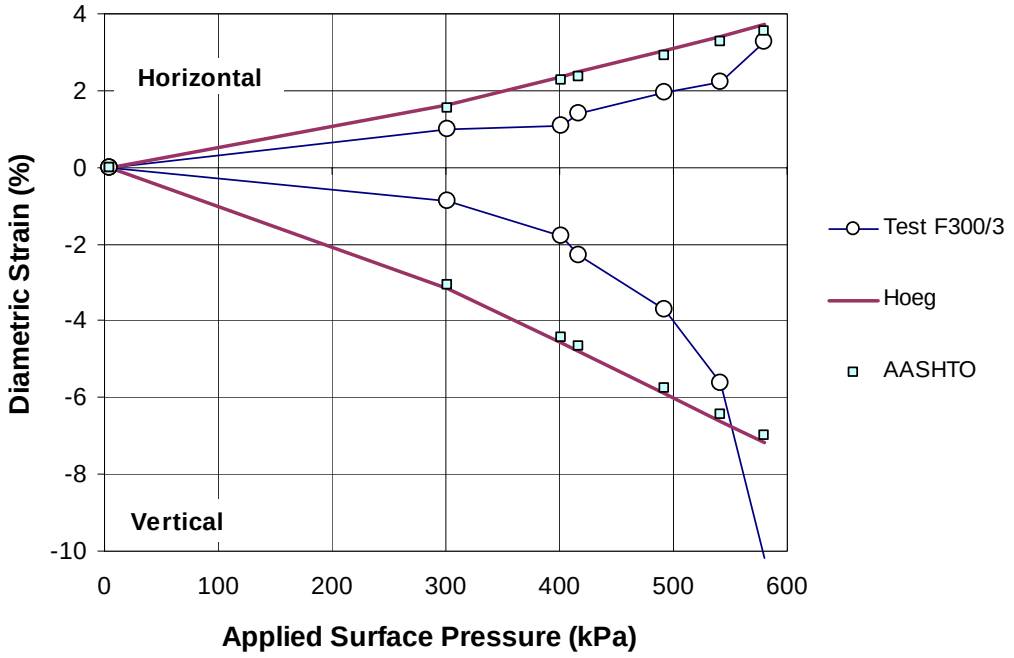

Figure 9-37. Vertical pipe deflection estimates for field test, F300/3, based on Hoeg's theory and the estimated average vertical pressure above the pipe

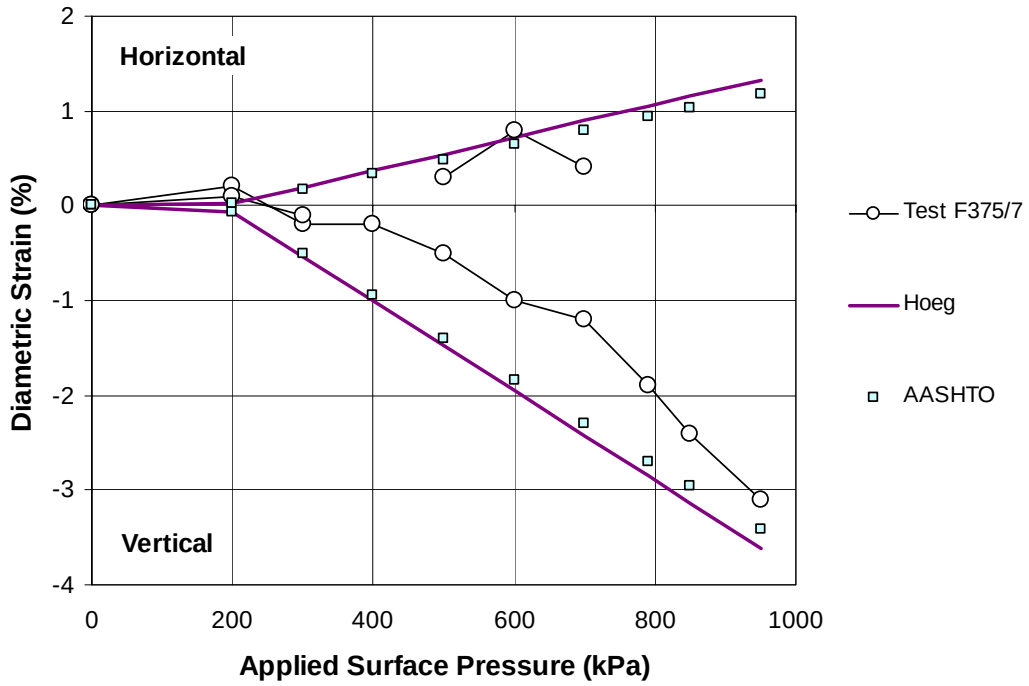

Figure 9-38. Vertical pipe deflection estimates for field test, F375/7, based on Hoeg's theory and the estimated average vertical pressure above the pipe

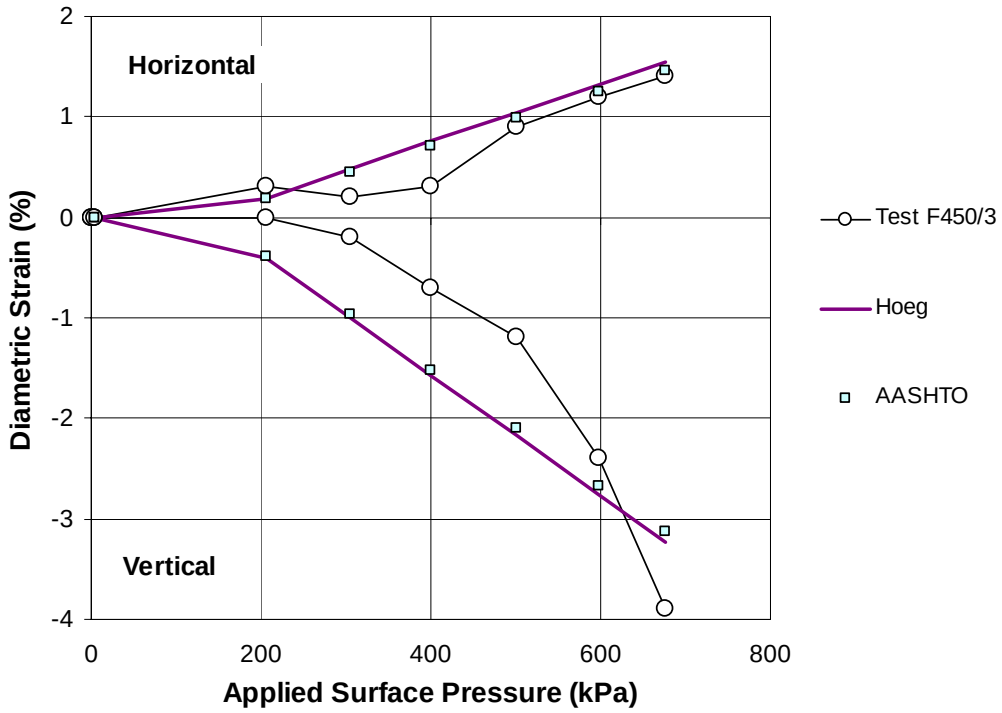

Figure 9-39. Vertical pipe deflection estimates for field test, F450/3,based on Hoeg's theory and the estimated average vertical pressure above the pipe

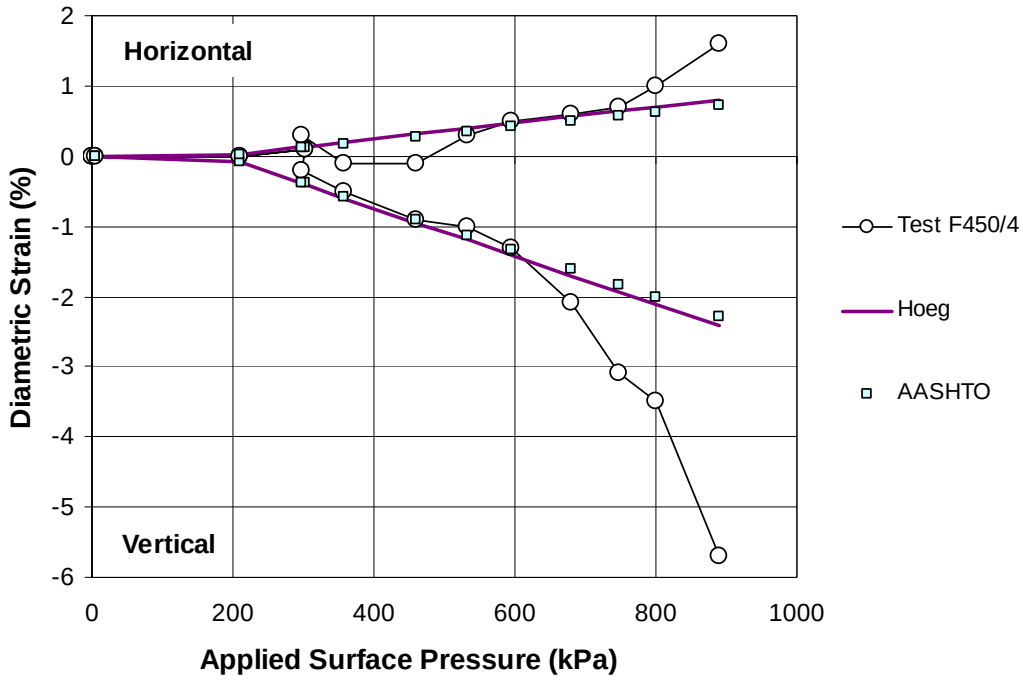

Figure 9-40. Vertical pipe deflection estimates for field test, F450/4, based on Hoeg's theory and the estimated average vertical pressure above the pipe